U.S. ARMY

U.S. ARMY COMBAT CAPABILITIES DEVELOPMENT COMMAND
CHEMICAL BIOLOGICAL CENTER
ABERDEEN PROVING GROUND, MD 21010-5424

DEVCOM CBC-TR-1900

Reactions of Neat HD with Li_3N+H_2O and Other Reagents for the Tactical Disablement Project

David J. McGarvey

RESEARCH AND OPERATIONS DIRECTORATE

William R. Creasy
Rachel Knoebel

Leidos, Inc.
Abingdon, MD 21009-1261

Mark K. Kinnan
Patrick D. Burton
Jeffery A. Greathouse
Susan L. Rempe
Calen Leverant
Chad Priest

Sandia National Laboratories
Albuquerque, NM 87123-3836

May 2024

Disclaimer

The findings in this report are not to be construed as an official Department of the Army position unless so designated by other authorizing documents.

REPORT DOCUMENTATION PAGE

1. REPORT DATE	2. REPORT TYPE	3. DATES COVERED	
		START DATE	END DATE
XX-05-2024	Final	Feb 2019	Sep 2021

4. TITLE AND SUBTITLE
Reactions of Neat HD with Li_3N+H_2O and Other Reagents for the Tactical Disablement Project

5a. CONTRACT NUMBER	5b. GRANT NUMBER	5c. PROGRAM ELEMENT NUMBER

5d. PROJECT NUMBER	5e. TASK NUMBER	5f. WORK UNIT NUMBER
CB10412		

6. AUTHOR(S)
McGarvey, David J. (DEVCOM CBC); Creasy, William R.; Knoebel, Rachel (Leidos); Kinnan, Mark K.; Burton, Patrick D.; Greathouse, Jeffery A.; Rempe, Susan L.; Leverant, Calen; Priest, Chad (Sandia National Laboratories)

7. PERFORMING ORGANIZATION NAME(S) AND ADDRESS(ES)
Director, DEVCOM CBC, ATTN: FCDD-CBR-PD, Aberdeen Proving Ground, MD 21010-5424
Leidos, Inc.; 3465 Box Hill Corporate Center Drive, Suite A, Abingdon, MD 21009-1261
Sandia National Laboratories; 1611 Innovation Parkway SE, Albuquerque, NM 87123-3836

8. PERFORMING ORGANIZATION REPORT NUMBER
DEVCOM CBC-TR-1900

9. SPONSORING/MONITORING AGENCY NAME(S) AND ADDRESS(ES)	10. SPONSOR/MONITOR'S ACRONYM(S)	11. SPONSOR/MONITOR'S REPORT NUMBER(S)
Defense Threat Reduction Agency, 8725 John J. Kingman Road, MSC 6201, Fort Belvoir, VA 22060-6201	DTRA	

12. DISTRIBUTION/AVAILABILITY STATEMENT
Distribution Statement A. Approved for public release: distribution is unlimited.

13. SUPPLEMENTARY NOTES
Parts of this report were previously published in the final project report:
U.S. Department of Energy Office of Scientific and Technical Information. CB10412: Bulk CWA Destruction (Technical Report) | OSTI.GOV (accessed 30 April 2024).

14. ABSTRACT
As part of the Tactical Disablement Project, neat weapons-grade HD was reacted with lithium nitride (Li_3N) and water in glass reaction containers. The reaction with HD was less successful than the reactions obtained with nerve agents in previous studies. Other reagents were studied for neutralization, and the most effective reagent was $NaOCH_3$. Products were analyzed to determine residual HD. Solid product was formed under some reaction conditions, but the ratio of reagents to HD did not meet the goals of the project. Ab initio computational studies were performed to generate data for comparing the reactions because HD has a complex chemistry that can involve S_N2 and E2 reaction mechanisms, nonpolar and ionic reaction intermediates and products, and cyclic sulfonium ion intermediates. Machine learning tools were reviewed to determine the methods that might be useful for modeling reactivity.

15. SUBJECT TERMS
HD NMR Sulfur Mustard Tactical Disablement Decontamination

16. SECURITY CLASSIFICATION OF:			17. LIMITATION OF ABSTRACT	18. NUMBER OF PAGES
a. REPORT	b. ABSTRACT	C. THIS PAGE		
U	U	U	UU	76

19a. NAME OF RESPONSIBLE PERSON	19b. PHONE NUMBER *(Include area code)*
Renu B. Rastogi	(410) 436-7545

STANDARD FORM 298 (REV. 5/2020)
Prescribed by ANSI Std. Z39.18

Blank

PREFACE

The work described in this report was authorized under project no. CB10412. The work was started in February 2019 and completed in September 2021.

The use of either trade or manufacturers' names in this report does not constitute an official endorsement of any commercial products. This report may not be cited for purposes of advertisement.

U.S. Army Combat Capabilities Development Command Chemical Biological Center (DEVCOM CBC) was previously known as U.S. Army Edgewood Chemical Biological Center (ECBC).

This report has been approved for public release.

Acknowledgments

The authors acknowledge the following individuals for their hard work and assistance with the execution of this technical program:

- Mr. Kevin Morrissey (DEVCOM CBC, Decontamination Sciences Branch; Aberdeen Proving Ground, MD) for contract support;
- Dr. Glenn Larson (Defense Threat Reduction Agency; Fort Belvoir, VA) for program support and discussions; and
- Mr. Todd M. Alam and Mr. Thomas Fisher for their contributions to the research effort (Sandia National Laboratories; Albuquerque, NM).

Blank

CONTENTS

FIGURES

TABLES

REACTIONS OF NEAT HD WITH Li_3N+H_2O AND OTHER REAGENTS FOR THE TACTICAL DISABLEMENT PROJECT

ABSTRACT

As part of the Tactical Disablement Project, neat weapons-grade HD was reacted with lithium nitride (Li_3N) and water in glass reaction containers. Reaction with HD was less successful compared to nerve agents used in previous studies. Other reagents were studied for neutralization, and the most effecting reagent was $NaOCH_3$. Products were analyzed to determine residual HD. Solid product was formed under some reaction conditions, but the ratio of reagents to HD didn't meet the goals of the project. A*b initio* computational studies were done to indicate a wealth of information for comparing reactions, since HD has a complex chemistry that can involve S_N2 and E2 reaction mechanisms, nonpolar and ionic reaction intermediates and products, and cyclic sulfonium ion intermediates. Machine learning tools were reviewed to determine which methods might be useful for modeling reactivity.

1. INTRODUCTION

The objective of the tactical disablement project is to use a minimal amount of reagents to make bulk chemical agent (CA) unusable as a threat through the neutralization and/or solidification of the bulk agent. This would ideally be done by performing reactions in the CA storage container via chemical reagents in order to avoid transporting the storage container or transferring the chemical out of the container into a reactor. The reaction would also ideally react to completion without any mechanical mixing, excessive agitation of the container, or external heating.

It is anticipated that the container will have at least 10% of the volume as empty headspace to allow for thermal expansion of the agent fill, so 10% was the target amount of additive reagents. By trying to utilize the CA storage container as the batch reactor, the logistical resources that are needed for decontamination can be significantly reduced. Fewer personnel are required since no sophisticated equipment needs to be set up, configured, or operated. Employing the CA storage container as the reaction vessel enables the capability to add reagents to multiple containers in a short period of time, as opposed to processing one container at a time for typical flowing reactor approaches. In scenarios where a quick response is required, the material can be added to all the CA containers and left to react on their own without intervention. This approach does not require sophisticated equipment, fuel, electricity to power equipment, or large quantities of decontamination materials. It does not generate a large amount of waste that must be transported and treated.

Neutralization is required to greatly reduce the toxicity of a CA. However, it is not anticipated that the toxicity will be completely eliminated by an environmentally approved decontamination such as the kind that was required for the destruction of the U.S. CA stockpile. As a result, this study didn't require a method for trace detection of residual HD in the reaction

products. It also didn't require a detailed kinetic study to determine how long it would take to reach a target amount of decontamination.

Formation of solid product can interfere with dispersal or nebulization of the CA, preventing its use as a weapon. Early concepts of the project involved efforts to form a solid polymer product. For example, incorporation of the CA into a reagent such as an epoxy could produce a solid polymerized matrix. However, it was found that simpler reagents could be used to form solid products. The solids were characterized by several analytical chemistry methods. A previous study of the characterization of solid products from VX reaction has been published.[1]

This study examines the neutralization and solidification of bulk mustard (HD) CA in a glass jar to simulate a storage container. The target for the minimal quantities of chemical reagents were typically 15% by weight of the amount of CA. The amount of reagent was set based on the stoichiometry of the reaction and by the addition of enough reagent to form a solid product. This didn't meet the target amount of 10% of reagent to CA. There is a possibility that removal of some agent to make enough volume for the addition of reagent might be unavoidable.

Reaction of several reagents were studied for the Tactical Disablement project. The most effective reagent for the purposes of the study in general was found to be lithium nitride and water ($Li_3N + H_2O$) for reactions of VX,[1] GB,[2] GD,[3] QL,[4] and DF.[5] This reagent was very effective in decontaminating these nerve agents and precursors by basic hydrolysis. It also formed a solid product that made the agent into a form that couldn't be easily dispersed or used for military purposes.

However, HD is significantly less polar and has different chemistry from the nerve agents and precursors, and the reaction of $Li_3N + H_2O$ was studied for HD but it was not an effective reaction. A survey of other reagents was done. The most effective reagent for destroying HD in neat solution was found to be sodium methoxide ($NaOCH_3$). However, this reagent was not effective in small amounts specified for the goal of the project. Some reaction studies were done with simulants of HD.

In addition to experimental trials, computational studies were done at Sandia National Laboratories to investigate the energetics of reactions of potential reagents.

2. SURVEY OF REACTION STUDIES

2.1 Reactions with $Li_3N + H_2O$

Li_3N was selected as a reagent due to its strong basicity (after reacting with water to form LiOH) and low molecular weight, even though it is not widely used as an aggressive synthesis reagent.[6 7] The reaction of $Li_3N + H_2O$ forms lithium hydroxide and ammonia (or ammonium hydroxide),[8] according to the reaction [9]:

$$Li_3N + 3H_2O \rightarrow 3LiOH + NH_3 \text{ (aq or gas)}$$

These products react by caustic hydrolysis with the agent. The major product that is expected is thiodiglycol for HD hydrolysis reaction. It is important to note that the reactions can get very hot during the early stages of reaction if water is added directly and quickly to the Li_3N. Microbubbling could be due to boiling or outgassing of the water or CA. (Much more boiling was observed in larger reaction volumes, as discussed later.) It doesn't appear that enough gas is generated to indicate that a large amount of ammonia is lost as vapor. As a result, it seems likely that most ammonia is in solution in the form of ammonium hydroxide, a strongly basic compound.

Several small-scale studies were done on the reaction of HD with Li_3N. The HD was from U.S. Army Combat Capabilities Development Command Chemical Biological Center (DEVCOM CBC) Chemical Agent Standard Analytical Research Material (CASARM) program, and it was checked for purity by NMR before use. Lithium nitride (Li_3N) was purchased from Sigma-Aldrich (MilliporeSigma, St. Louis, MO), P/N 399558-25G. Water was from an in-house distillation system.

Test reactions were done in Nuclear Magnetic Resonance (NMR) glass sample tubes that could be analyzed directly by NMR. Other reactions were done in small vials, and samples of the liquid or solid product were removed, weighed, dissolved or extracted with chloroform, and analyzed by NMR. Signals for HD peaks were compared to a known amount of an internal standard, 1,1,1,2-tetrachloroethane.

2.1.1 $Li_3N + H_2O$ Powder

When HD was added to Li_3N solid without water, no reaction was observed. When water was added, there was heat and pressure due to reaction of the water with Li_3N. When the reaction was sampled for quantitation, there was still 80 wt% of the original HD left and no reaction products were observed. A vial from a 1 mL volume of HD is shown in Figure 1. A solid formed from the reaction products, but most of the HD is still present.

However, for one of the reaction runs (sample number NB097P89B), the reaction mixture reacted rapidly and formed a charred black solid mass when 36% w/w reagents were added, shown in Figure 2. No reaction products were extracted from the residue and no HD was extracted either. It is possible that the $Li_3N + H_2O$ reaction was hot enough in this case to cause reaction or evaporation of the HD. It was observed in experiments with DMMP that a reaction between Li_3N and pure water can cause the Li_3N to become red hot under some circumstances, which can be hot enough to ignite combustion.[10] When repeating the reaction at lower quantities (22% w/w) of reagent, the reaction did not proceed that way, and no reaction was observed.

It was difficult to reproduce or identify the conditions that are necessary to perform this kind of reaction. Since water doesn't dissolve in the HD, it may have reacted more vigorously with the reagent powder as they both floated to the top of the HD. It is also possible that the H_2O was added faster to this sample. It isn't clear what caused the reaction with the HD to form charred residue, and it doesn't seem that it can be done reproducibly or under safe, controlled conditions.

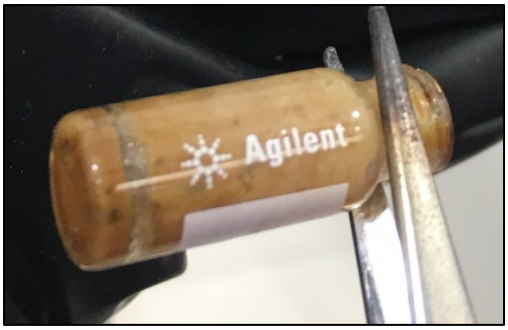

Figure 1. Reaction mixture of HD with $Li_3N + H_2O$ (22% w/w), sample NB097P143D.

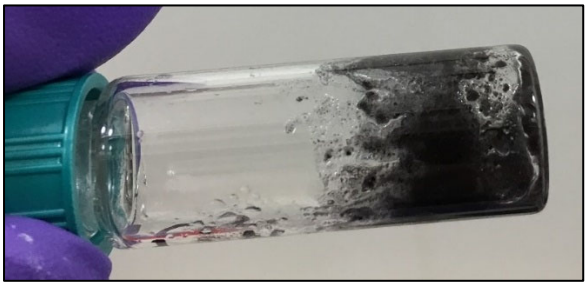
Figure 2. Reaction mixture of HD plus $Li_3N + H_2O$ (36% w/w), sample NB097P89B.

2.1.2 1.2 $Li_3N + H_2O$ Tablets

Pucks or tablets of Li_3N were made at Sandia National Laboratories (SNL) by compressing Li_3N powder, sometimes with an additive to provide cohesiveness. Tablets consisting of 9% w/w $LiAlH_4$ dispersed in Li_3N were pressed and sent to DEVCOM CBC to determine if the $LiAlH_4$ aided in breakup of the Li_3N tablet into powder. Tablets were expected to make the Li_3N easier to transport and add to a container, and less hazardous to the operator. They also may control the reactivity by decreasing the surface area compared to a powder.[2]

The reactivity of Li_3N pucks was evaluated with a simple method of monitoring pH and temperature when the puck was added to water. Each puck, approximately 0.3 g, was added to 50 mL of deionized (DI) H_2O and monitored with an Orion VersaStar temperature corrected pH probe. The probe output (both pH and temperature) was continuously monitored during the reaction, and in one case, for an extended period after reaction. When the pellet was added, an effervescent reaction began almost immediately that generated a steady stream of gas bubbles. The exothermic production of LiOH caused an increase in pH to ~12.5, and a corresponding temperature increase (Figure 3). The unbuffered solution remained at high pH as the solution cooled in a subsequent extended test (Figure **4**).

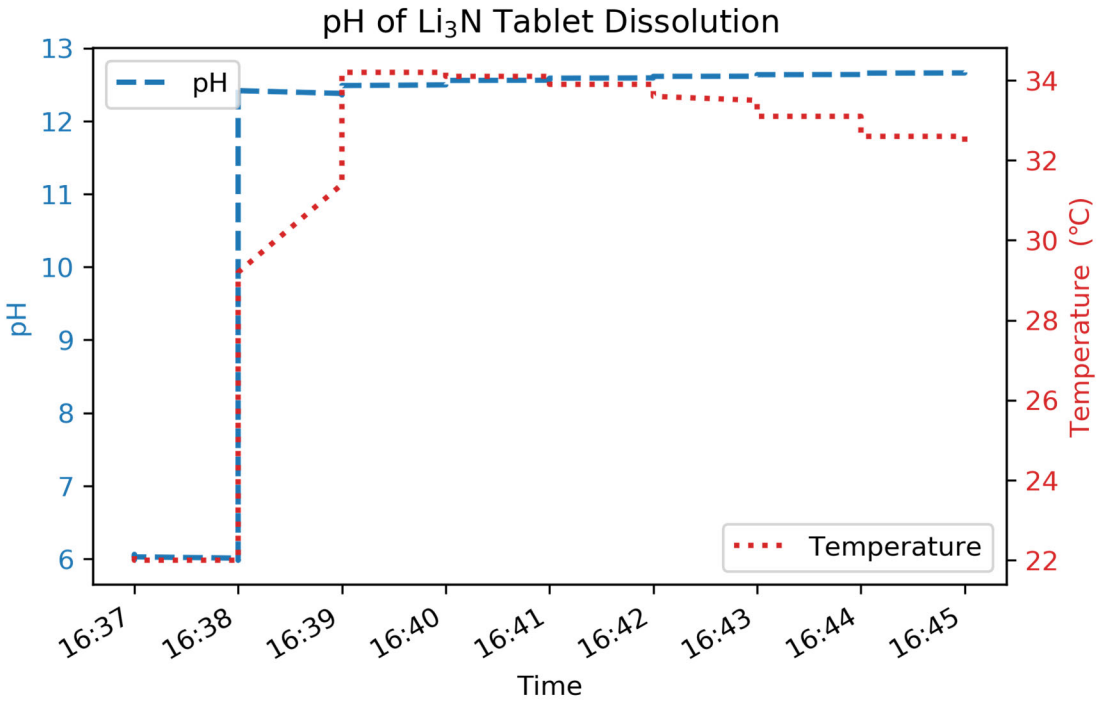

Figure 3. pH (left axis) and temperature (right axis) increase upon addition of Li_3N puck to 50 mL DI H_2O.

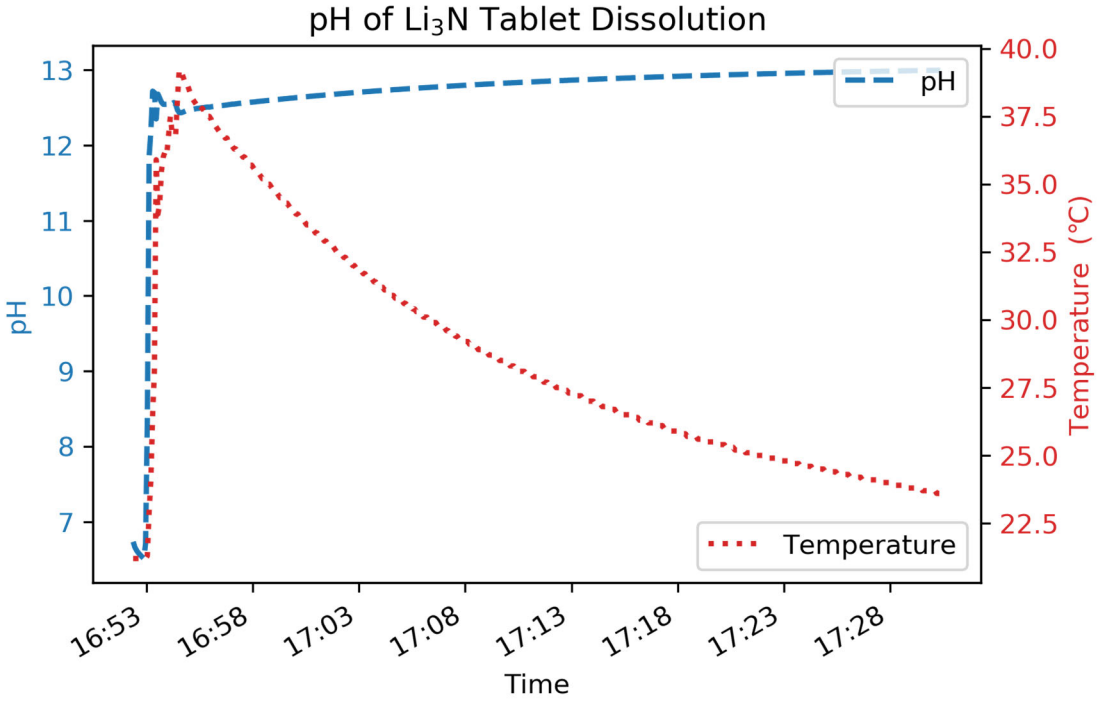

Figure 4. Extended monitoring of Li_3N dissolution after puck was fully consumed. Once the reaction was complete, the solution returned to room temperature while the pH remained constant.

The efficacy of pressed Li_3N pellets was compared to a similar mass of loose powder in bis(chloroethyl)ether (BCEE), a less toxic simulant of HD. A pellet (0.0425 g Li_3N) and 0.0480 g Li_3N powder with 1000 µL BCEE each were mixed with water on a 3 eq basis to Li_3N. After no initial reaction was observed in either vial, successive aliquots of water (100, followed by 1000 µL) were added to achieve a reaction. The powder sample began to effervesce and a distinct phase separation was noted. The pellet sample did not visibly react, but the liquid clouded over time.

Further reaction optimization was undertaken at SNL using BCEE. Since the pellet did not remain in good contact with water due to differing density and solubility, an effort to increase the aqueous solution density was made. A saturated solution of potassium carbonate (K_2CO_3, 112 g in 100 g DI H_2O) was used to improve liquid contact with the pellet, as shown in Figure 5.

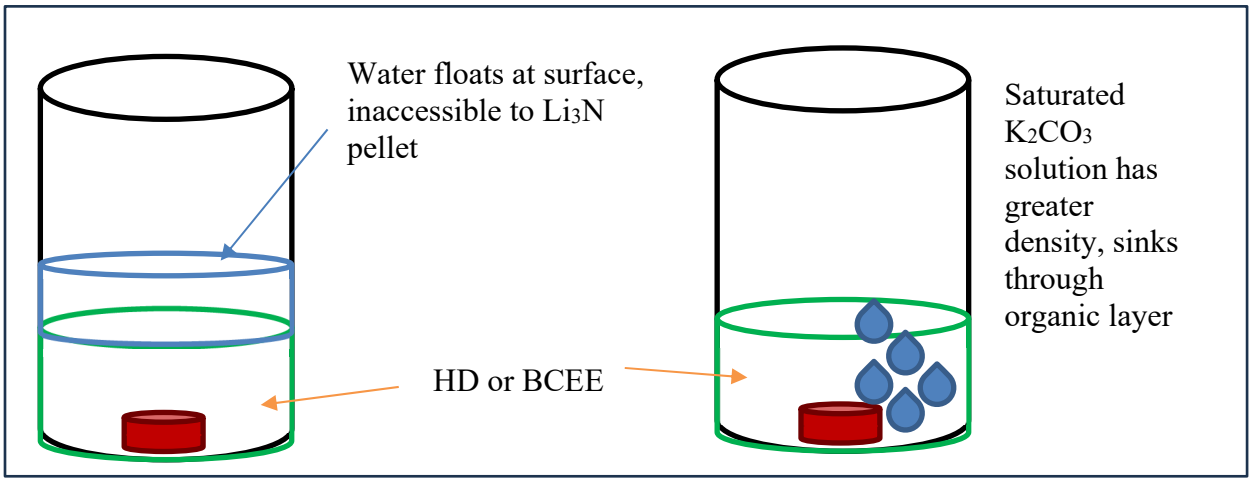

Figure 5. Illustration of using high density salt solutions to overcome mixing limitations of water and BCEE.

Initial efforts with potassium chloride had limited success, as the solution did reach the pellet, but did not substantially react with the Li_3N. A second attempt with saturated K_2CO_3 was more successful. K_2CO_3 is highly soluble in water, to a literature value of 112%. K_2CO_3 produces a moderately basic solution (pH 10-11), which can enhance the hydrolysis rate.

2.1.3 Reactions of $Li_3N + H_2O$ with Mixed Solvents

Studies were done using 10% of H_2O as a reagent and 20-30% propylene carbonate as a co-solvent for studies of HD reaction. The reaction mixture formed some solid, and the liquid appeared to be a single layer. However, a considerable amount of HD remained, so the reaction didn't go to completion.

Experiments were done using Li_3N pellet with an aqueous solution of Fe(II) acetate as a catalyst. Another experiment was done using Li_3N pellet with triethanolamine as a multifunctional alcohol. This could also be formed as a reaction product of Li_3N with ethylene glycol. No reaction was observed.

It is possible that further studies along these lines of inquiry would lead to a combination of solvents that would be reactive with HD. However, finding a combination that reacted quickly at room temperature appeared to be a complicated problem. The issue of the density of HD compared to aqueous solutions seems to have been solved by using a salt solution.

The hydrophobicity of HD makes it difficult to find a water-based decontamination agent. This is not unexpected, since the chemistry of HD has been studied in many previous studies.[11 12 13] It was found that the rate of hydrolysis of HD with water was usually limited by the rate of solvation of HD in water. The current reaction conditions are different for most previous studies in having an excess of HD rather than excess aqueous solution, so the HD functions as a solvent. It was not initially clear whether HD could dissolve a useable amount of water for a slow reaction, or whether it could react directly with Li_3N solid, but it was found that the reactions don't meet the project requirements.

2.1.4 Reactions of Protonated Solvents

Non-aqueous solvents were tested for further improvements in reactivity, density matching, and miscibility with BCEE. Simple alcohols, ranging from short chain lengths (methanol) to surfactant-like (dodecanol) were used as the solvent and Li_3N reaction activator. Reactivity with the Li_3N powder was inversely proportional to chain length, with methanol producing a violent reaction, and dodecanol producing no immediately perceptible reaction. The reaction with alcohols was expected to produce lithium hydroxide and the corresponding alkylamine, shown in Figure 6. Polyols, including propylene glycol and glycerin, were used as reagents to improve miscibility and produce multidentate alkylamines as a product. Viscous mixtures of solvent afford some degree of control and miscibility with Li_3N, as they do not immediately react on contact.

Analysis of reaction products via Raman spectroscopy indicated partial consumption of the surrogate. Raman spectra were collected on a Thermo-Fisher (Nicolet) DXR SmartRaman with a 780 nm source.

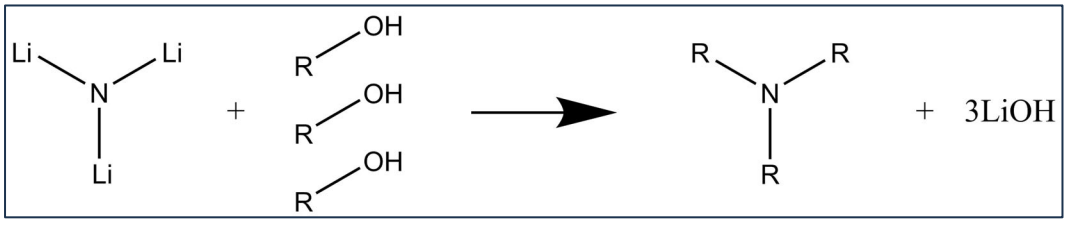

Figure 6. Reaction of lithium nitride and alcohols.

Methanol as an organic solvent in place of water was found to be an effective reagent to activate Li_3N. The solubility of HD and simulants should be higher in methanol and

other alcohols than water. Additionally, the alkyl products produced from hydroxyl cleavage should produce alkylamines as opposed to ammonia. The alkylamines were expected to be more reactive and have better miscibility than gaseous ammonia.

Reactions using methanol as the solvent were effective for the decomposition of chloroethyl phenyl sulfide (CEPS), as monitored by the decline of a C-Cl peak via Raman spectroscopy, shown in Figure 7. A greater reaction rate was achieved with more Li_3N and sodium dodecylsulfate (SDS) as a surfactant to the solution. Methanol, ethanol and an equimolar mixture were used as solvents in comparison to water, all with added SDS to enhance solubility. The ethanol/SDS solution exhibited the greatest decrease in the chlorine peak.

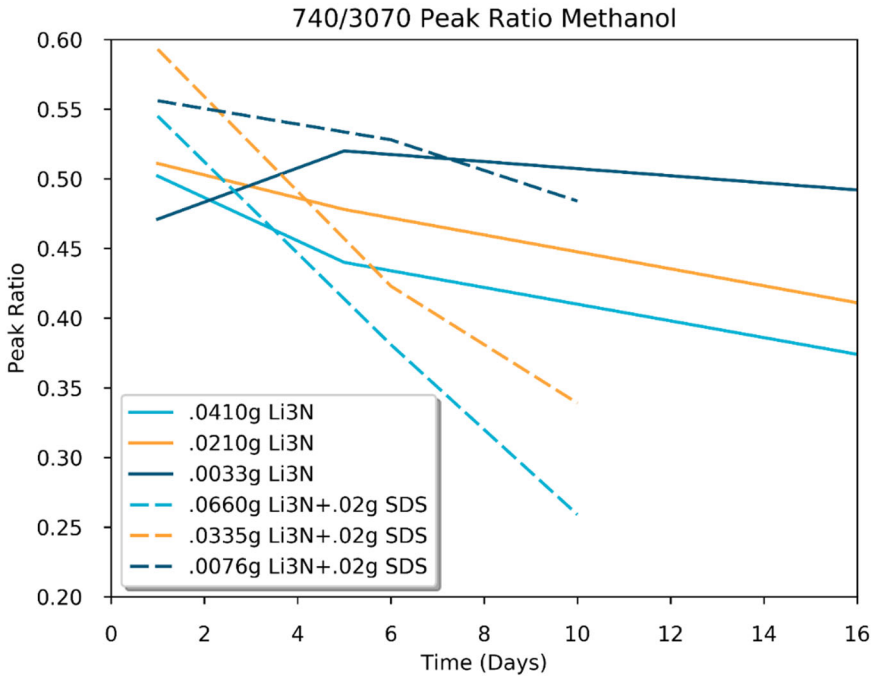

Figure 7. Peak ratio of C-Cl to C-OH peak measured by Raman spectroscopy for methanol at varying ratios of Li_3N. Neat solvent reactions are shown in solid lines, and solvent with surfactant reactions are shown in dashed lines.

Other solvent/reagent mixtures were evaluated to find an effective means to solubilize and react simulants. Pyridine was considered a candidate to function both as solvent and reagent via the cyclic amine functional group. In place of water, a solvent mixture of pyridine and methanol was added to Li_3N and BCEE. The alcohol was expected to activate the Li_3N, and the pyridine was expected to serve as a solvent and additional amine source. In contrast to typical reactions between Li_3N and water, this reaction was mild. No noticeable exothermic behavior occurred. After reacting overnight, the entire system formed a translucent gel, as shown in Figure 8. In order to further elucidate reaction behavior, neat pyridine was added to BCEE. A pink solution developed and evolved to dark red after 16 hours, eventually

resulting in a dark red precipitate, shown in Figure 9. A subsequent reaction with a small amount (5 vol%) of water reduced the reaction rate, resulting in a pink color only after 5 days. Extraction with water or hexane resulted in the pink solution migrating into the aqueous phase.

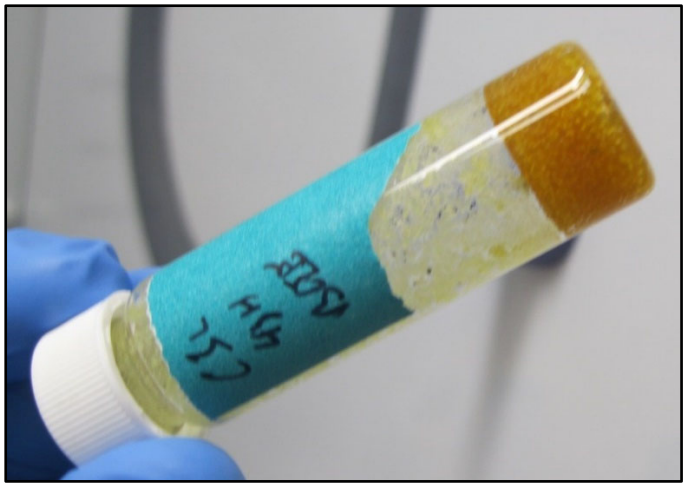

Figure 8. Gelled BCEE/Li_3N/py/MeOH reaction after reacting overnight. Typical LiOH reaction products (grey/white powder) did not form.

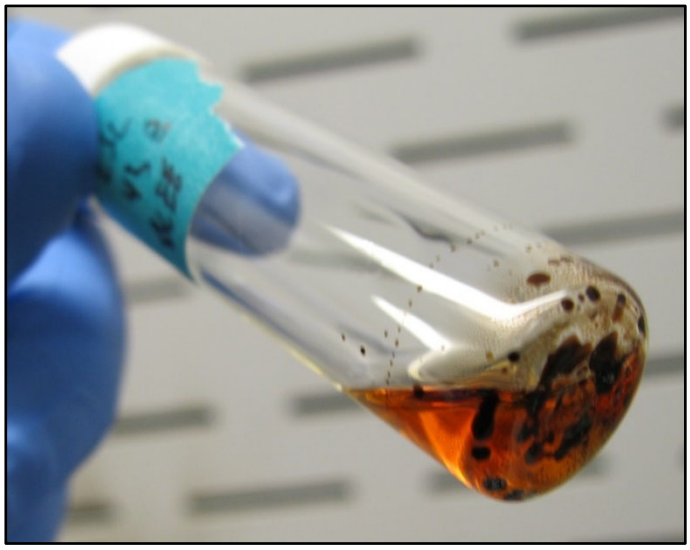

Figure 9. Neat BCEE/py reaction after 5 days showing dark red coloration and solid precipitates.

Other amine-containing reagents were investigated, including urea and thiourea. Thiourea presented a particularly appealing approach, as the reaction product (oxygen urea) could itself further react with HD. It is possible that this could result in polymerization of the HD. While some color change was observed, no change was detectable by Raman spectroscopy. Reaction vials are shown in Figure 10.

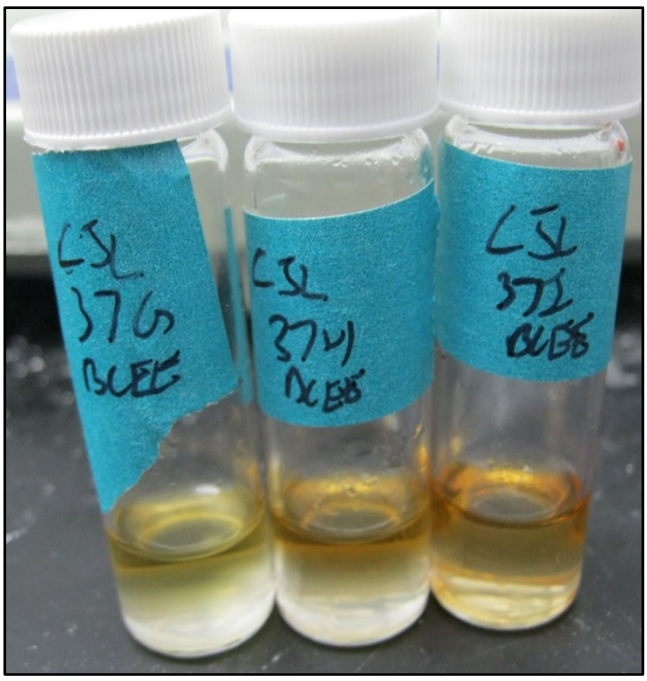

Figure 10. Reactions of BCEE with Li_3N and thiourea. The solution developed an orange coloration but did not polymerize or exhibit other signs of reaction.

In addition to S_N2 nucleophilic substitution of HD by Li_3N and reaction products, E_2 elimination may also be possible. In this scheme, shown in Figure 11, ammonia or other nucleophile reacts with hydrogen on the alkyl carbon, displacing terminal chlorine and generating a C=C bond. This reaction mechanism is more likely under strongly basic conditions. Notably, this mechanism does not involve a sulfonium ion intermediate. Formation of a vinyl end group may initiate polymerization.

Reaction conditions were tested using KOH solution to vary the pH values from 9, 11, and 13. Control solutions were tested in parallel following the same conditions, without Li_3N. The Li_3N and BCEE were mixed before adding alkaline solution dropwise. The reaction rate of the Li_3N was proportional to solution pH. The pH 9 solution produced irregular, step-wise off-gas events with the Li_3N; the pH 11 solution produced more steady results, and the pH 13 solution yielded consistent reactions, allowing a steady dropwise addition of the aqueous solution. The product solutions were extracted with hexane and examined using Raman spectroscopy. No substantial consumption of the reactions was observed, shown in Figure 12. The poor reaction performance was attributed to limited solubility of BCEE in aqueous solution. Despite highly reactive alkaline conditions with elevated temperature (from Li_3N decomposition), the bulk of BCEE remained unreactive.

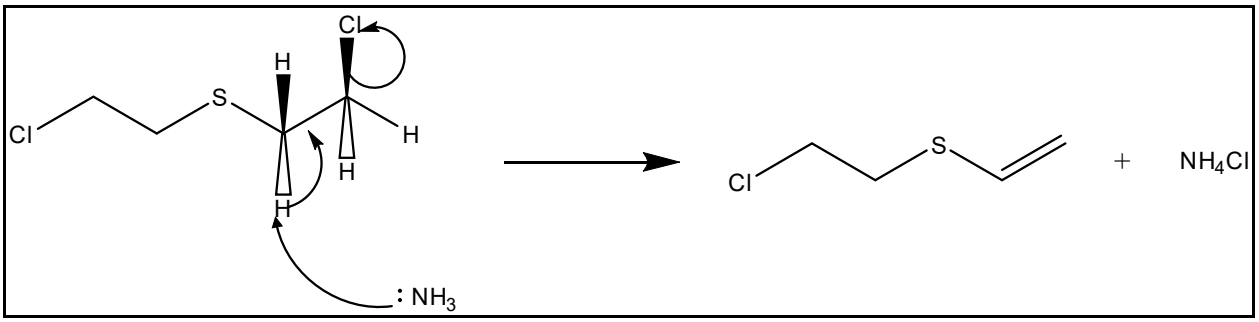

Figure 11. E2 elimination possible mechanism generating a vinyl sulfane.

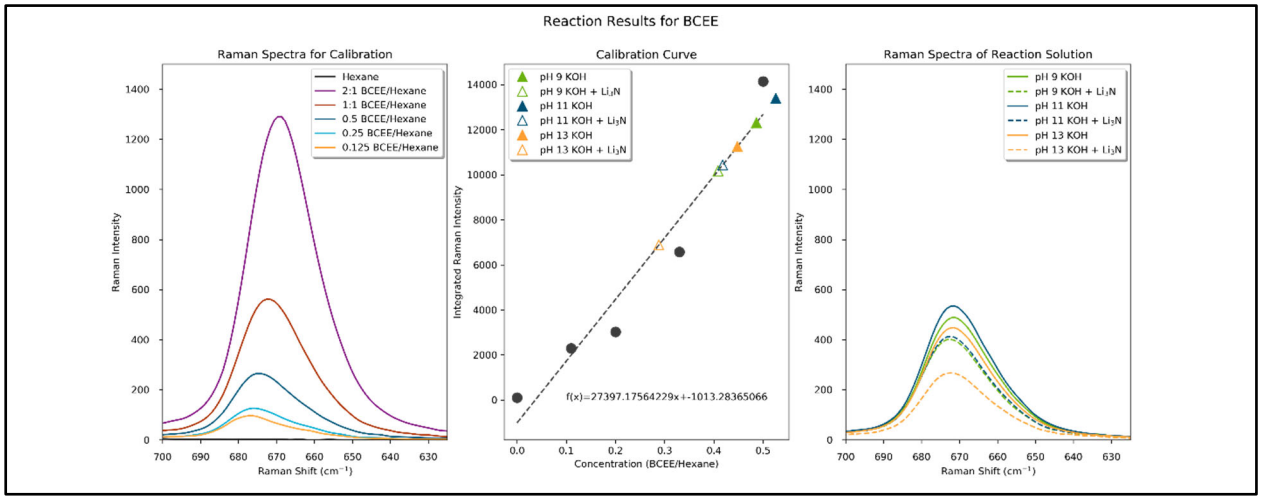

Figure 12. Raman spectra and calibration curve for pH reaction series. Nominal extraction is 0.33 BCEE:hexane.

On analysis of these results, aqueous solubility appears to remain a challenge for the E2 (and S_N2) reactions. A non-aqueous basic solvent, such as was attempted with pyridine (see Figure 9) may be more favorable for elimination reactions than substitution reactions.

Since low molecular weight alcohols are effective for activating Li_3N, diethylene glycol (DEG) should likewise provide sufficient hydroxyl groups to react with the Li_3N. A trial sample consisting of equal volumes BCEE and DEG was added to Li_3N. The reaction was significantly less vigorous than typical water or alcohol reactions with comparable amounts of Li_3N. A subsequent test was mild enough to allow for pH monitoring via moistened test strip placed at the mouth of the vial. Highly alkaline conditions were noted immediately. An amine-containing volatile gas was evolved without the presence of water. Aqueous hydrolysis in pH 9, 11, and 13 solutions was repeated, with the addition of 30 wt% H_2O_2. Since BCEE dissolved in its own hydrolysis product, improved miscibility with the aqueous solution was anticipated. Unfortunately, the continuing production of hydrolysis product/solvent was not sufficient to solubilize the BCEE, and the emulsion broke upon addition of the alkaline oxidizing solution. Figure 13 shows reaction products from Li_3N with propylene glycol and methanol using an equimolar mixture.

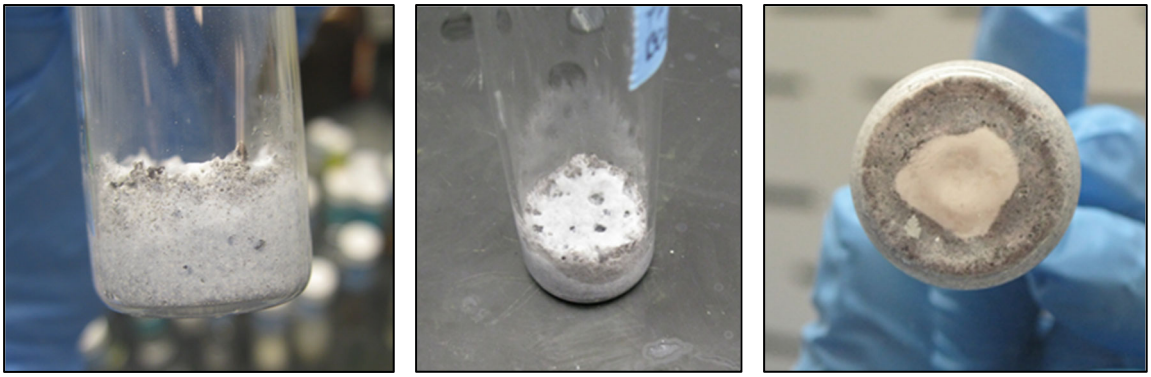

Figure 13. Images of reaction product from Li_3N with propylene glycol and methanol equimolar mixture.

Diethylamine (DEA) was also studied as a multifunctional reagent and solvent, since it is miscible with BCEE. As a secondary amine, it is a good nucleophile for abstracting chlorine ions from the surrogate. DEA thus achieves the two necessary conditions for reaction.

When mixed in a stoichiometric ratio (1 mole BCEE to 2 moles DEA), a crystalline precipitate develops after many hours, shown in Figure 15. Increasing the ratio of DEA corresponds to greater consumption of BCEE, shown in Figure 14, but oddly less formation of the crystalline solid. Triethylamine is similarly miscible with BCEE, but less reactive.

Formation of a solid crystalline product, and in some cases a yellow color, indicated ongoing reaction progress over several days. In Figure 16, a series of volumetric reactions using (from left to right in each image) 1:1, 1:0.75, 1:0.5, 1:0.25, and 1:0.125 BCEE:DEA progressed from 1 to 7 days. Development of crystalline deposits was more rapid in vials with more DEA. A yellow tint developed first in the vials with the least DEA, but eventually was observed in all vials. Figure 17. Vials containing 2:1, 1:1 and 1:2 ratios of BCEE:DEA.

Based on these results, it is likely that the DEA forms a quaternary product (2-(2-chloroethoxy)-N,N-diethylethan-1-aminium chloride {BCEE-$HNEt_2$}) when reacted with BCEE, shown in the scheme in Figure 18. The quaternary product of triethylamine and BCEE (2-(2-chloroethoxy)-N,N,N-triethylethan-1-aminium chloride {BCEE-NET_3}) is carbon saturated and cannot react further. In experiments using triethylamine, no crystalline solids were observed, only a color change (yellow) indicated any reaction progress at all. In contrast, the BCEE-$HNEt_2$ has one remaining reactive proton, and can further react with BCEE. A charged oligomer may result from successive reaction steps, shown in Figure 18.

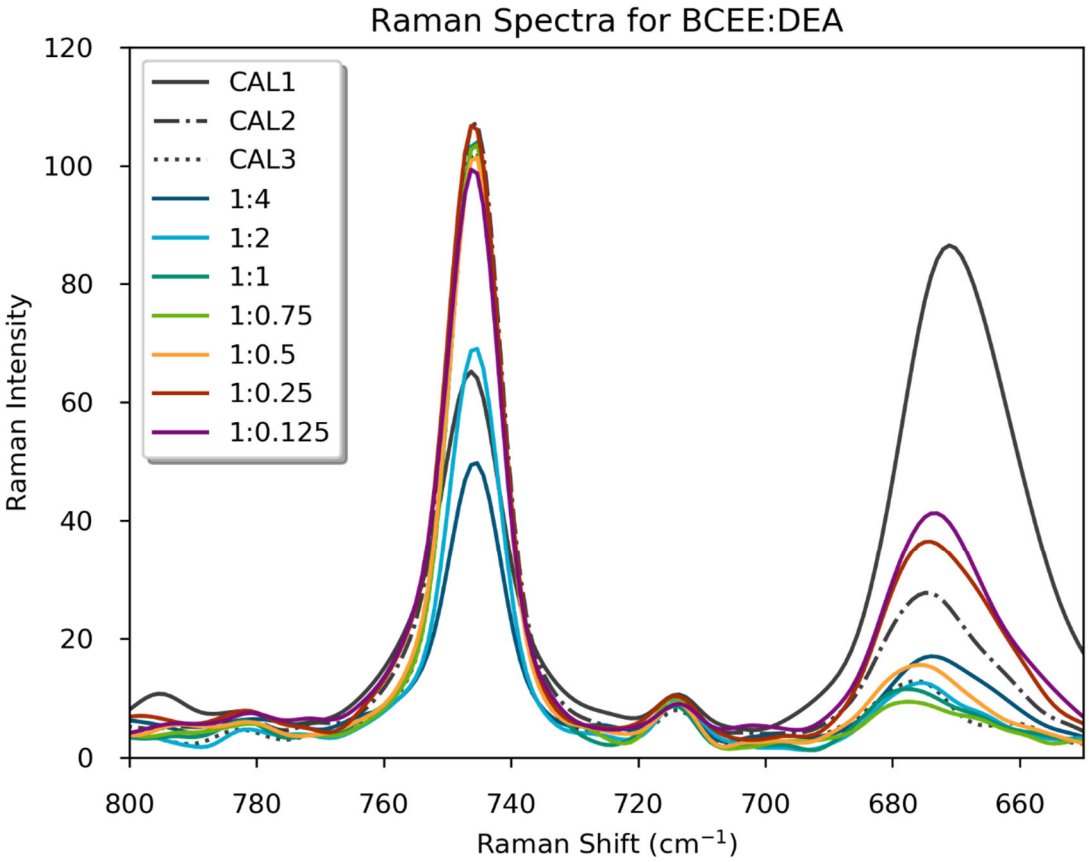

Figure 14. Raman spectra of serial dilutions of BCEE and diethylamine (DEA). Reduction in BCEE correlated to concentration of DEA.

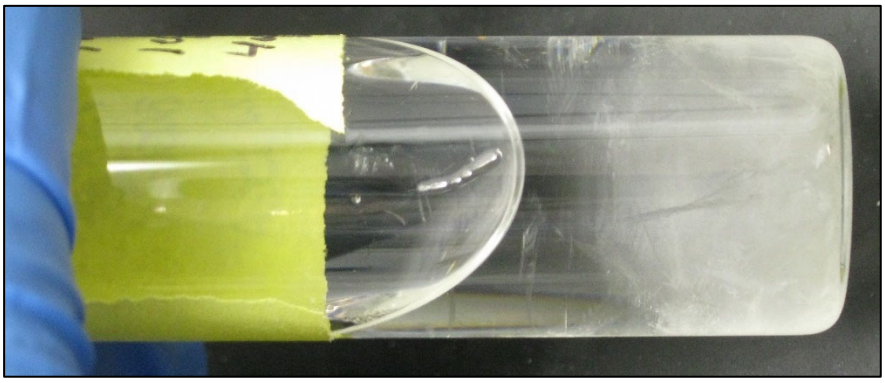
Figure 15. Mixture of BCEE and DEA (1:4 ratio) showing formation of fine needle-shaped precipitates.

Figure 16. Series of BCEE:DEA mixture ratios after several days; (left) 1 day, (right) 7 days.

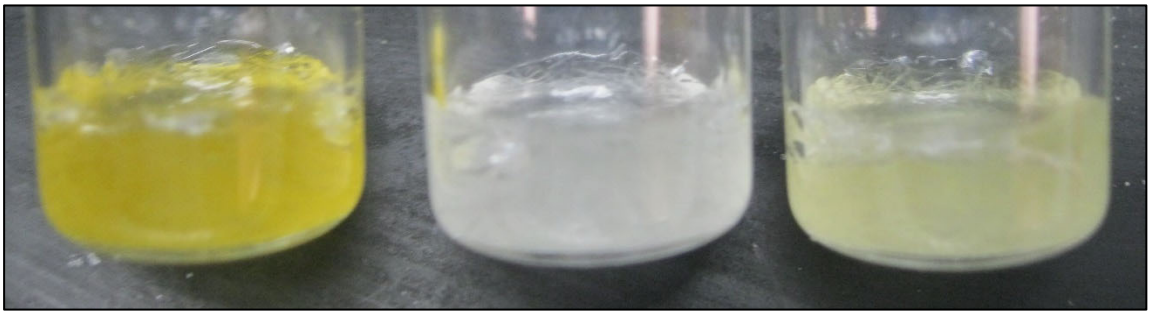

Figure 17. Vials containing 2:1, 1:1 and 1:2 ratios of BCEE:DEA.

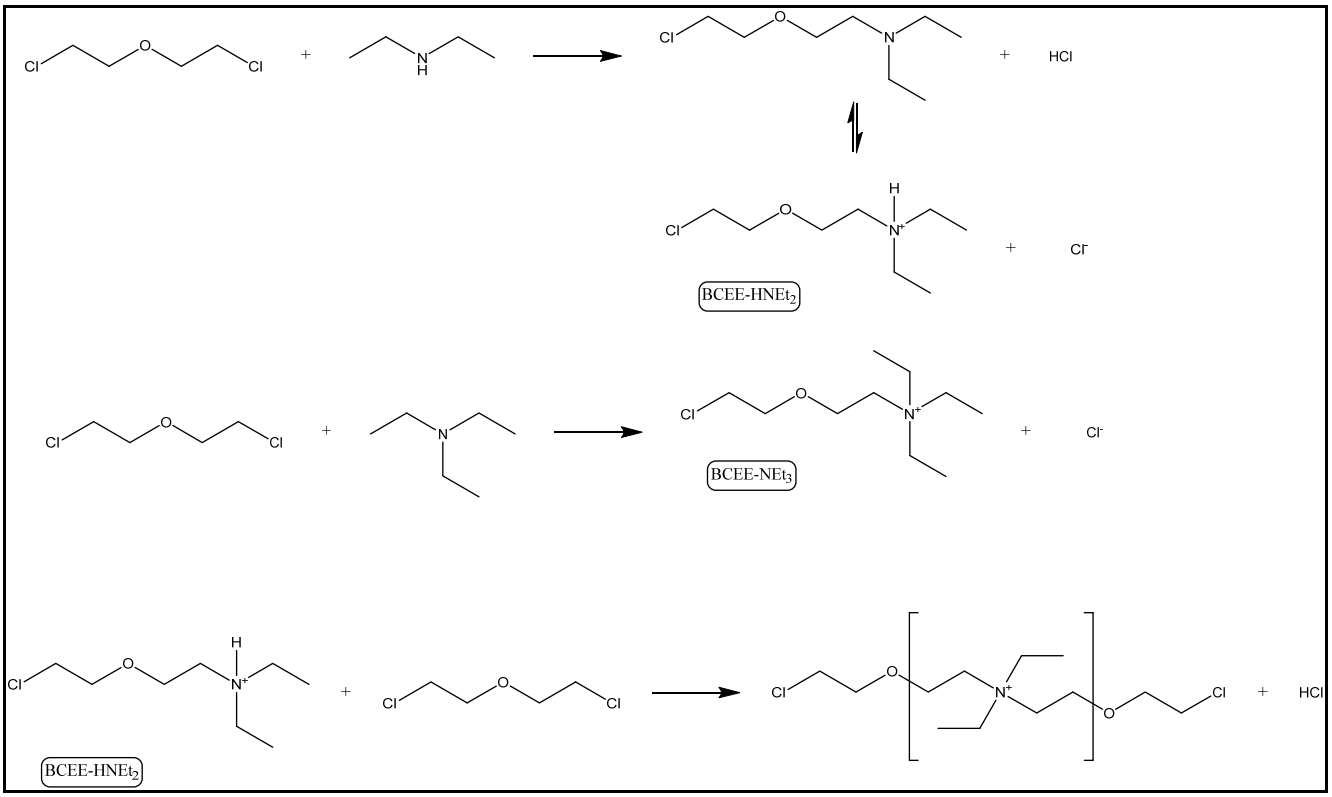

Figure 18. Proposed reaction scheme of BCEE and DEA forming a quaternary amine product.

Use of dimethylamine as a solvent and reagent has shown some success but is not entirely sufficient to completely consume BCEE, shown in Figure 19. The reaction progresses by the formation of crystalline deposits and eventual orange color development. However, some amount of starting reagent was consistently found in the recovered product. Additives, such as isopropanol, have resulted in similar semi-crystalline products. Interestingly, addition of isopropanol resulted in precipitation of large, flat platelets instead of the typical needle-shaped crystals. The isopropanol may form a complex or otherwise determine the structure of the final product.

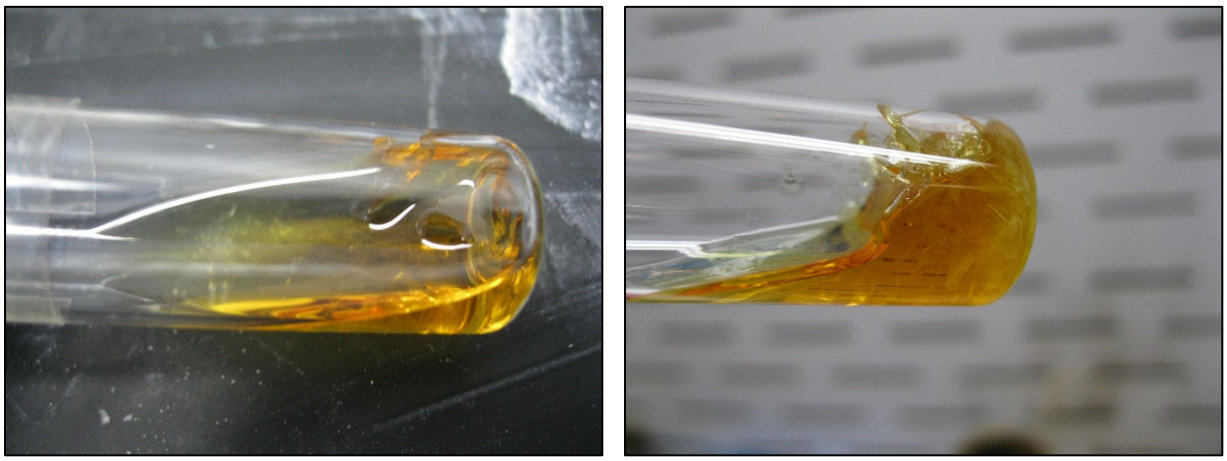

Figure 19. BCEE reacted with DEA and isopropanol (left) after 24 hours and (right) after 6 days. Platelet crystals were observed floating after 24 hours and had grown to a substantial portion of the entire volume after 6 days.

Diethylamine has not been independently effective at fully reacting with BCEE. It was investigated as a solubility enhancing agent for reaction with Li_3N, and other additives. Pressed pellets of Li_3N were submersed in a mixture of BCEE and equimolar DEA/IPA. After an initial reaction period where small bubbles (presumably ammonia) were generated, the pellet developed a layer of LiOH. Further dissolution was not observed, and likely obstructed by the LiOH layer, shown in Figure 20.

Fumed silica was also added to DEA as a means to better homogenize and stabilize the mixture with BCEE. An apparently completely solidified product was obtained. Residual BCEE was extracted by adding hexane to the post-reaction product and recovering a light-yellow solution.

Additional efforts to improve the dispersion of reactive chemistry into the simulant included a solution of ferric chloride in ethanol. A two-phase separation was initially observed, but the solution homogenized easily with moderate agitation.

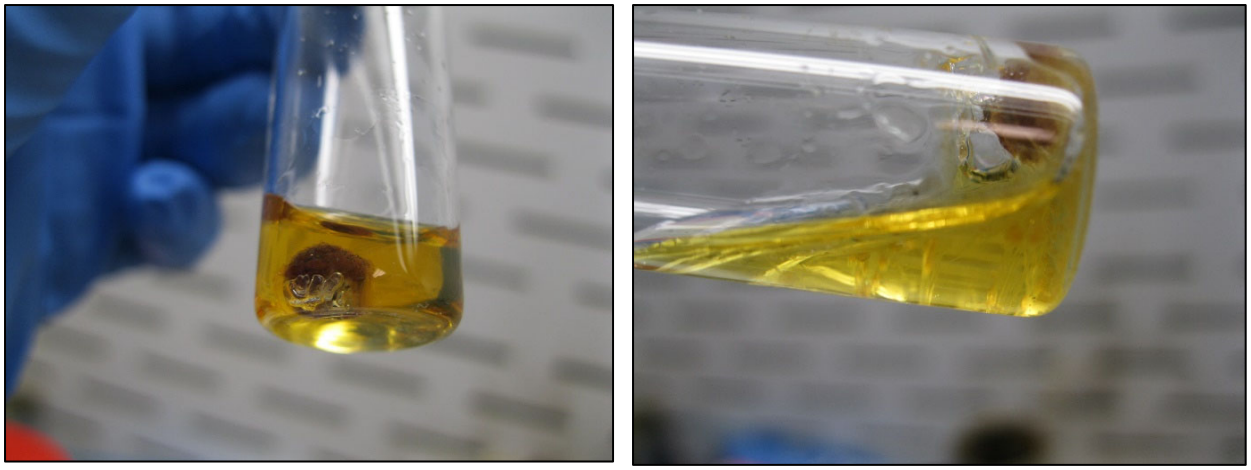

Figure 20. Li3N pressed pellet after 24 hours (left) and 6 days (right) exposure to DEA/IPA solution.

A compatibility test between BCEE and $MgCO_3$ as a loose powder (unpressed, not fabricated as part of the pellet) showed they didn't react. Lithium nitride pellets were submerged in the vial with saturated potassium carbonate solution as the reaction initiating water source. A two-phase region developed as the water displaced BCEE. The pellets floated at the brine/surrogate interface. A very faint wispy stream of white precipitate evolved. After an additional two weeks, the pellets had been fully consumed. A companion study was conducted under similar conditions with the addition of diethylamine to the initial reaction mixture. The liquid solidified over night without addition of Li_3N, Figure 21 (left). After reacting for five days, the entire bulk material turned an opaque peach color, Figure 21 (right).

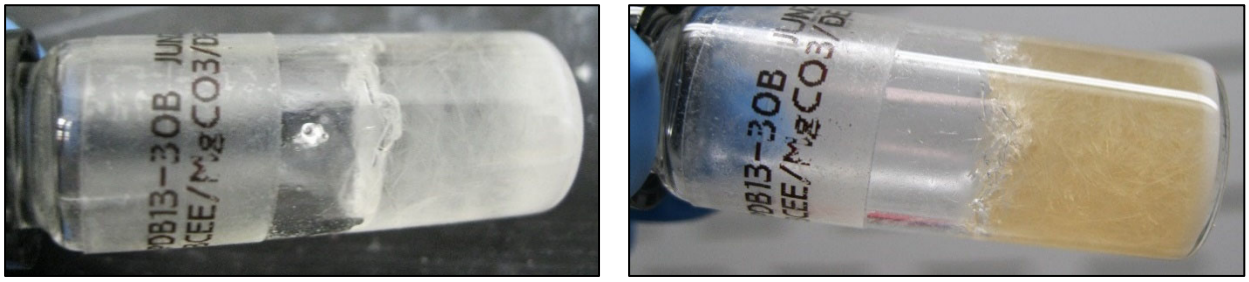

Figure 21. BCEE reacted with $MgCO_3$ and diethylamine after 18 hours (left) and 5 days (right).

Pellets were subsequently fabricated using $MgCO_3$ and Li_3N. The solids were mixed together prior to pressing in a die press. Pellets were added to 1 mL BCEE and 1 mL isopropanol. Dehalogenation of the surrogate would produce hydrochloric acid, which could subsequently react with $MgCO_3$ in order to consume HCl, shift equilibrium, and potentially generate an active $Mg(OH)_2$ product. Evolution of CO_2 gas should aid mixing, akin to ammonia production from Li_3N. The reaction was conducted in alcohol instead of water to limit aqueous side reactions. Two separate batches of Li_3N were used, one having been air exposed during storage. The aged material reacted slowly (Figure 22 left), while the fresher sample (Figure 22 right) reacted within minutes. Extent of reaction propagation remains a concern, as some material remained unreacted (red layer at bottom of vial, Figure 22 right).

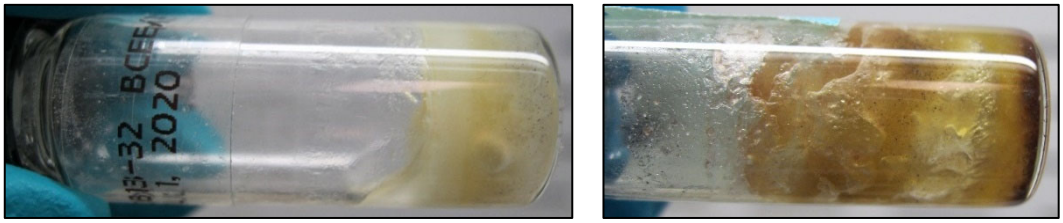

Figure 22. Comparison of aged (left) and new (right) lithium nitride reactivity.

Stoichiometric ratios of $MgCO_3$ and Li_3N were evaluated. Equal mass trials were prepared in which the Li_3N:$MgCO_3$ molar ratio was 1:0, 1:1, or 1:2. A total of 0.49 g material was added to 1 ml BCEE, with the relative molar composition of each powder scaled accordingly. Water was added to each reaction on the basis of 3 equivalents of Li_3N. Due to the low volume of water, reactions were not complete. The 1:1 molar ratio appeared solid but was a viscous slurry; it did appear to fully react as no Li_3N was visible. Larger mass scale-up reactions did not produce well-homogenized results, shown in Figure 24.

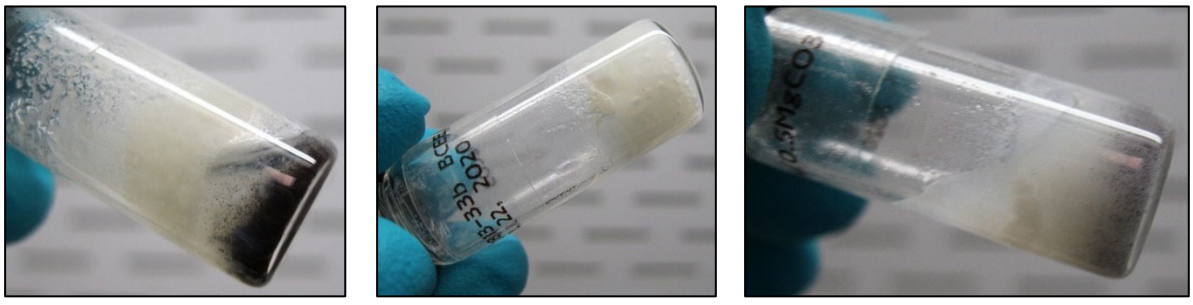

Figure 23. Reactions of BCEE, Li_3N, $MgCO_3$, and water. Li_3N:$MgCO_3$ molar ratio was 1:0 (left), 1:1 (middle), or 1:2 (right).

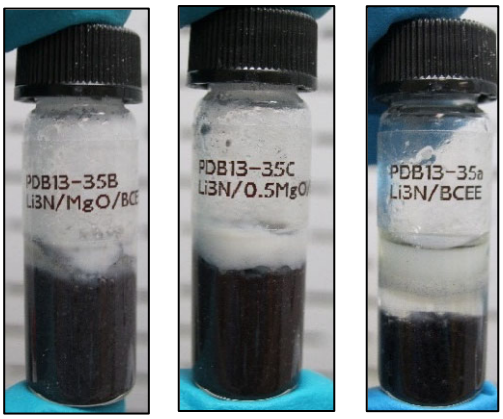

Figure 24. Scaled up reactions of BCEE, Li_3N, $MgCO_3$, and water. Li_3N:$MgCO_3$ molar ratio was 1:0 (left), 1:1 (middle), or 1:2 (right).

2.1.5 Additional Pellet Studies

Fabrication of pellets proceeded without solid additives. Exploratory efforts found that a wax binder was not needed in order to produce a dense, robust pellet under atmospheric conditions. Similar results could not be achieved in an inert glovebox. Demonstration pellets could also not be fabricated under inert atmosphere. Water vapor was estimated to produce some binding effect for the powder.

Substitute organic binders were evaluated. Diethylamine (DEA) was considered as a dual function binder and reagent. Pellets could be produced when sample powder was wetted with DEA under benchtop conditions. A small amount of liquid was expelled when the wetted powder was pressed. Pressed pellets were minimally reactive when tested with BCEE and saturated potassium hydroxide solution. A surface layer evolved over time, and the aqueous phase developed a yellow tint, shown in Figure 25.

Wax dissolved in hexane was tested as a substitute binder. However, despite dissolving the wax into solvent, it could not be uniformly dispersed through the powder. Fabricated pellets had inconsistent amounts of wax left after immersion in water, Figure 26.

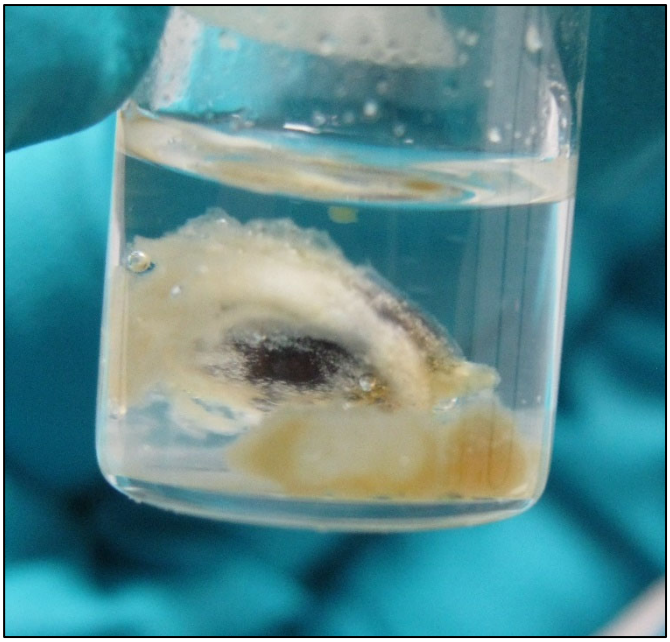

Figure 25. Demonstration of a Li_3N/DEA pressed pellet.

Figure 26. Li_3N/Wax pellet not fully dissolved.

Neat solvents (hexane and 2,3,5-trimethylpentane) were explored next. Similar results were achieved as with the DEA. Excess liquid was expelled from the press. When immersed in water, the pellets were slow to react. Diffusion of the non-polar solvent out of the pellet was observed. Since the solvents were not miscible with water, it was possible that the solvent could prevent water from reaching the surface of the pellet. Non-polar organic binders were thus determined to be incompatible with the eventual use of the pellets. Water-miscible

organic solvents, such as polyethylene glycol, were briefly considered. A demonstration test with Li_3N and 400 MW polyethylene glycol mixed overnight initially was unreactive but had begun to evolve gas by the following morning.

Ambient air pellet fabrication was determined to be the most effective means to produce Li_3N pellets. Fabrication in an inert (no oxygen or water vapor) atmosphere was not feasible without a binder. Since no suitable organic binder could be found, ambient moisture was determined to be suitable. The bulk storage container was maintained in an inert environment, and small aliquots were withdrawn, pressed into pellets, and then returned to the glovebox for inert storage conditions.

The extent of reaction in contact with brine (NaCl or KCl solutions) was evaluated with pellets fabricated in air. A drop of fluorescein dye was added to the brine to enable visual differentiation of the aqueous phase and organic simulant, diphenyl chlorophosphate, DPCP. The brine, prepared from NaCl in water, was not dense enough to sink through the surrogate. After five days, the entire volume solidified (Figure 27). A follow-on test was conducted using KCl brine with fluorescein dye applied directly to the surface of an immersed pellet. No immediate reaction was observed, although BCEE began to turn cloudy after about 10–15 minutes. After four days, the pellet remained intact, but had noticeable residue remaining on the surface, shown in Figure 28.

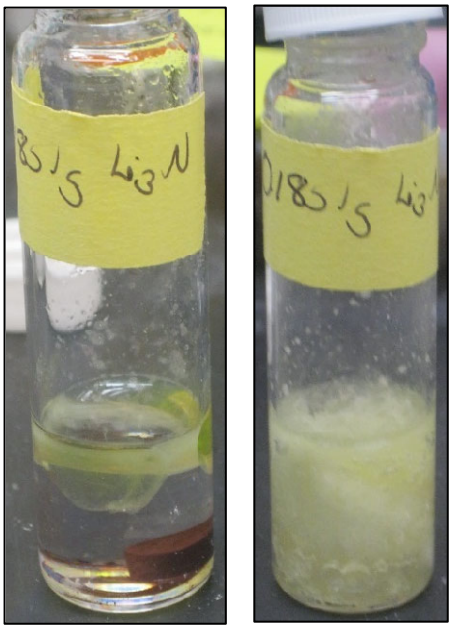

Figure 27. Brine sample as-prepared (left) and aged five days (right).

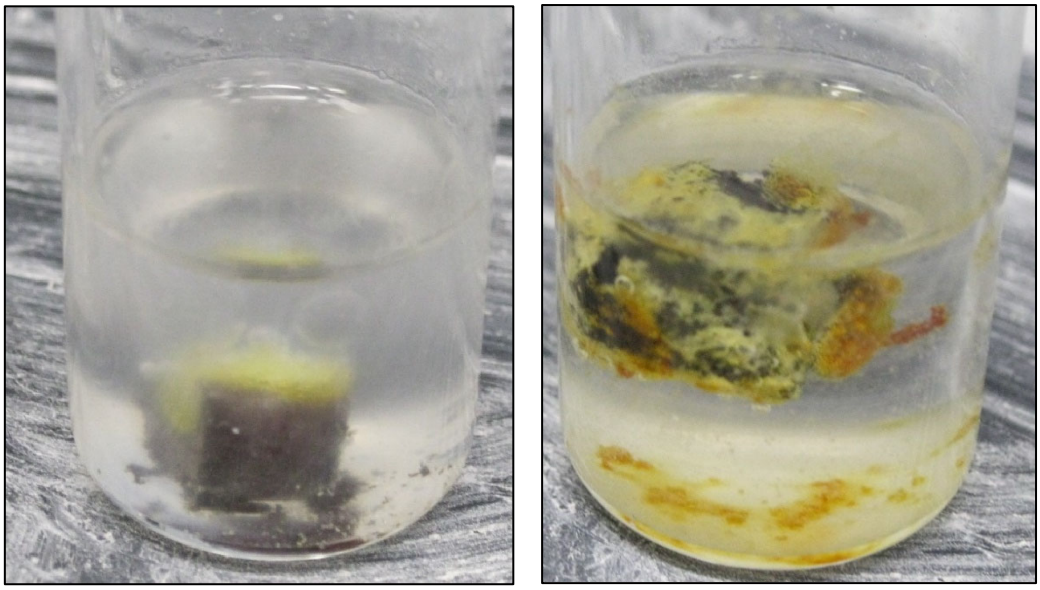

Figure 28. KCl brine with fluorescein dye applied directly to surface of a submerged pellet. Minimal reaction after four days.

The decomposition of Li_3N wetted with DPCP before contact with water was substantially slower than the decomposition of pellets added directly to pure water. The effect of pellet morphology and agitation was investigated to determine if mixing or diffusion was the cause. Replicate vials of Li_3N powder and DPCP, one stirred and one left quiescent, were tested with dyed KCl brine. The brine was added dropwise to each vial, whether stirred or not. Minimal reaction was observed in either vial. The brine remained near the surface of both vials, as shown in the photo in Figure 29. Some viscous behavior was noted in both vials, although no visible exothermic reaction occurred.

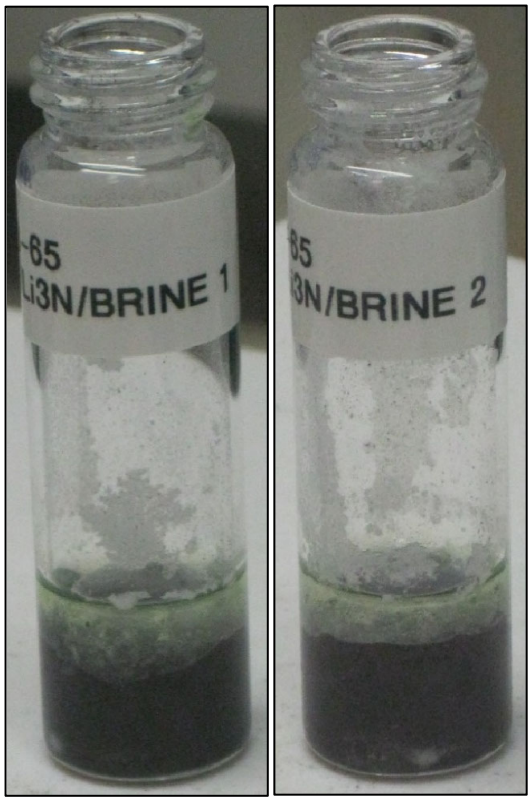

Figure 29. Quiescent (Brine 1, left) and stirred (Brine 2, right) reactions of DPCP and Li_3N powder with dyed KCl brine.

The presence of a variety of salts may impact hydrolysis of the simulants. Hydrolysis tests of DPCP in various salt solutions were conducted. Solid NaCl in DPCP was unreactive; but a mixture of 0.27 g NaCl in 1 mL DPCP and 1 mL DI H_2O slowly solidified (≈1/2 by volume) after three weeks. A replicate trial using reduced water conditions (0.24 g NaCl, 0.1 mL DI H_2O, 1 mL DPCP) resulted in an opaque slurry (Figure 30) which eventually completely dried after three weeks.

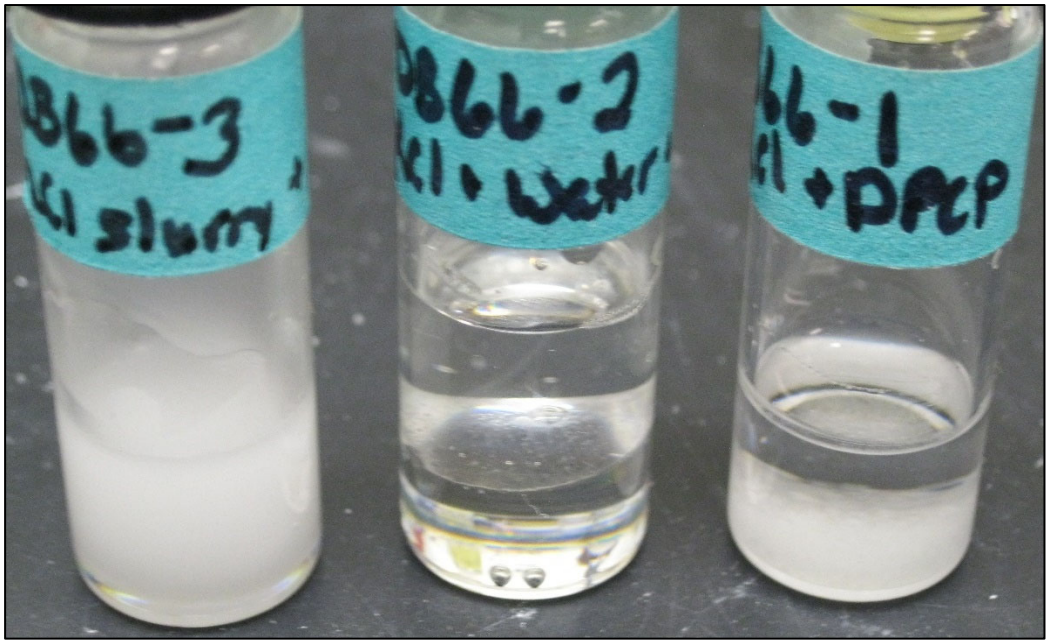

Figure 30. Sodium chloride brine hydrolysis tests with DPCP.

Similar tests were conducted with sodium citrate, resulting in a viscous, partially crystallized mixture. After three weeks, no free liquid remained in the vial (**Error! Reference source not found.**).

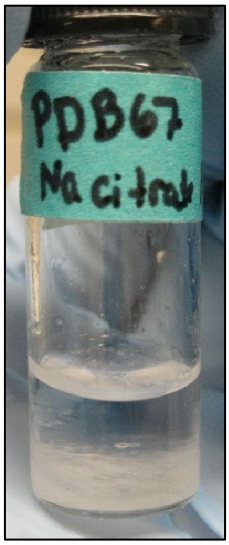

Figure 31.Sodium citrate hydrolysis test with DPCP.

Saturated NaOH and KOH tests were conducted with DPCP. After four days, the vial was entirely solidified, and needle-shaped crystals were growing from the solid surface

(Figure 32). Presence of salt products was evaluated to not be an interference with Li_3N decomposing DPCP. Inhibition of the Li_3N reaction with water was proposed as a possible cause of inconsistent reaction rates.

Figure 32. Fully solidified DPCP after four days exposure to a deliquescent slurry of NaOH flakes.

2.1.6 Studies of Li3N Chemistry

The decomposition product of Li_3N pellets was collected and analyzed via X-ray Diffraction (XRD) to determine phase composition. XRD spectra were collected on Bruker D2 Phaser with Cu Kα radiation. Spectra were indexed to International Centre for Crystallographic Data (ICCD) cards 01-087-0729 (Li_2CO_3), 01-074-6256 (Li_2O), 01-076-0911 (LiOH), and 00-025-0486 ($LiOH\cdot H_2O$).

In addition to the expected LiOH, Li_2CO_3 and LiO were identified as possible components (Figure 33). The presence of Li_2CO_3 may be due to reaction with atmospheric CO_2:

$$2LiOH + CO_2 \rightarrow Li_2CO_3 + H_2O$$

Accumulation of a surface layer of LiOH (or Li_2CO_3) was hypothesized as an inhibitory mechanism to the reaction of Li_3N with organic surrogates. A side reaction between carbonic acid from ambient CO_2 and water vapor was considered as a possible source of lithium carbonate noted in the decomposition product (see Figure 33).

$$2Li_3N + H_2CO_3 \rightarrow Li_2CO_3 + NH_3$$

Various carboxylic acids were tested to produce lithium carbonate on the pellet. Surface adsorbed carbonic acid was considered unavoidable and may lead to decreased overall reactivity of aged pellets. Citric acid was added to a test pellet of Li_3N in triethyl citrate as a complimentary organic phase. The pellet reacted vigorously to applied drops of acid solution and did not develop a grey surface coating. Additional solution continued to cause a fresh reaction. A second test adding neat citric acid solution to a Li_3N pellet resulted in a brief exothermic reaction but did not continue as more liquid was added. After five days, the fluid had gelled, and a small amount of Li_3N solid appeared to be entrained at the surface in froth.

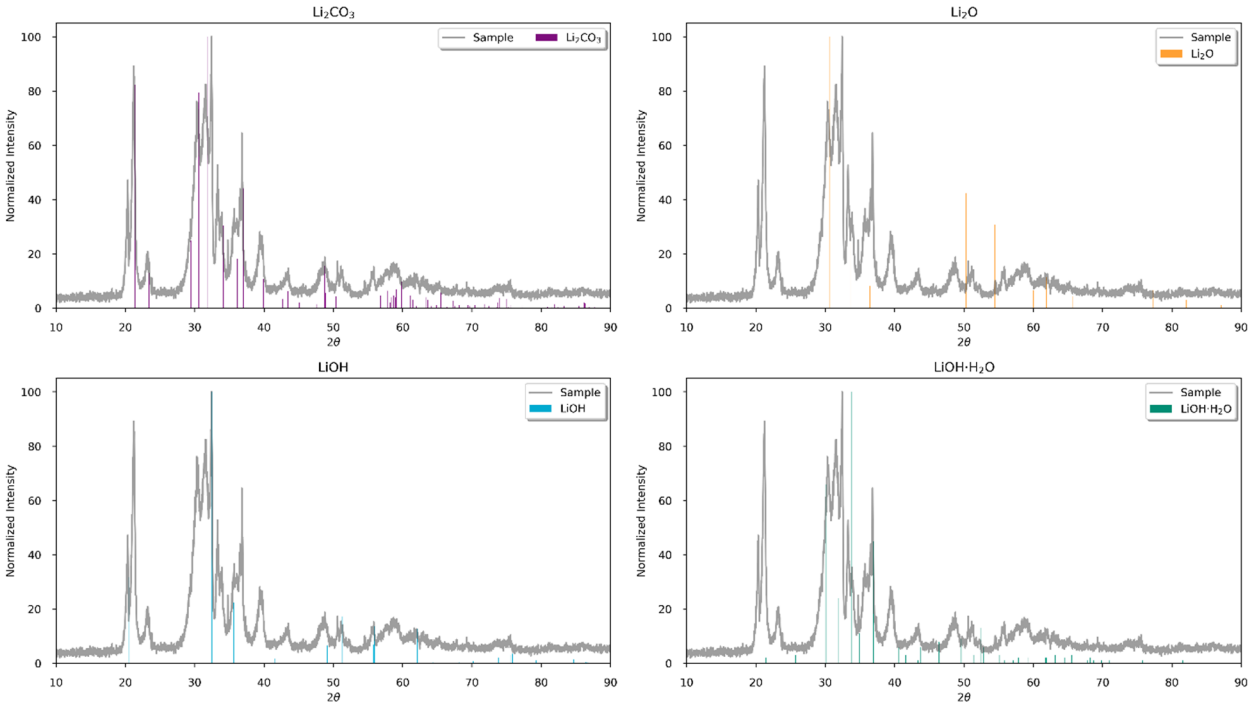

Figure 33. XRD plot of decomposed Li_3N residue. Plausible matches to LiOH, Li_2CO_3, weak match to Li_2O.

The physical configuration of the Li_3N pellet was considered as a possible contributing factor to the overall reaction rate. Delithiation of lithium nitride may have an intermediate energy barrier that can be more easily overcome when densely packed in a pellet. If the first delithiation step is much faster than the remaining two, a brief initiation followed by much slower kinetics could result in incomplete reactions. A dense pellet would provide more energy in a smaller volume, increasing the likelihood that subsequent reactions would progress.

$$Li_3N + H_2O \rightarrow Li_2HN + LiOH$$

$$Li_2HN + H_2O \rightarrow LiH_2N + LiOH$$
$$LiH_2N + H_2O \rightarrow H_3N + LiOH$$

A kinetics test was conducted with Li_3N powder uniformly stirred in hexane while water was added dropwise. The entire volume of dispersed powder reacted rapidly. Reaction kinetics are therefore unlikely to be impacted by pellet density.

Oleic acid was evaluated as an oily carboxylic acid to introduce reactive functional groups to the pellet while avoiding the miscibility problems associated with water. A pellet immersed in oleic acid with water added to the immediate surface reacted slowly. After twenty minutes, the surface of the pellet developed a grey layer. After two days, the liquid had reacted to form a fluffy white solid. Similar results were observed when reacting Li_3N pellets in oleic acid with acetone and isobutanol as oxygen-containing functional groups. Neat Li_3N powder was mixed with oleic acid in DPCP to test slow degradation activity. No immediate exothermic reaction was observed, but the previously colorless solution developed an amber tint after one week. The use of oleic acid as a Li_3N activator was further tested by immersing a pressed pellet in oleic acid, then adding to DPCP. No observable change occurred.

A validation experiment was conducted to corroborate findings at CBC[10] in which Li_3N pellets reacted in water above the liquid layer of agent. Despite the reaction occurring out of direct contact with the agent, or in a position for the produced ammonia to diffuse through the agent, solidification of the agent was observed. A benchtop experiment to replicate these results was conducted by placing an organic simulant in a vial, covering with water, and then adding a Li_3N pellet. Initial tests were conducted with triethylcitrate (TEC) as a physical analog to limit the possible unpredictable violent reaction. Various ratios of water to surrogate were tested while maintaining pellet mass at about 0.3 g in each trial. The pellet reaction time was proportional to the volume of water. In excess water (20 mL TEC, 10 mL H_2O), the pellet reacted rapidly and evolved a vapor plume that turned a witness pH strip blue. The plume is indicative of ammonia formation, and the pellet fully dissolved within a few minutes. A temperature change was evident, and some diffusion of aqueous solution into the organic layer was observed. Smaller volumes of water (25 mL TEC, 5 mL H_2O) resulted in incomplete reactions. At a minimum quantity of (30 mL TEC, 2 mL H_2O), the pellet was initially exothermic, but stopped reacting quickly. Despite the presence of water, the remaining Li_3N did not react.

It was postulated that equilibrium conditions of the aqueous phase limited the further production of LiOH. It is likely that excess accumulation of LiOH, rather than insufficient water, is responsible for incomplete reactions observed at CBC. In practice, adding excess water dilutes the LiOH concentration sufficiently to allow the Li_3N decomposition to proceed. Adding other solvents that can dissolve LiOH and improve miscibility with organic liquids would be favorable. Battery electrolytes, such as propylene carbonate, are one possible option. Another may be Cyrene™, a cycloether used as a greener alternative to DMF (Figure 34).

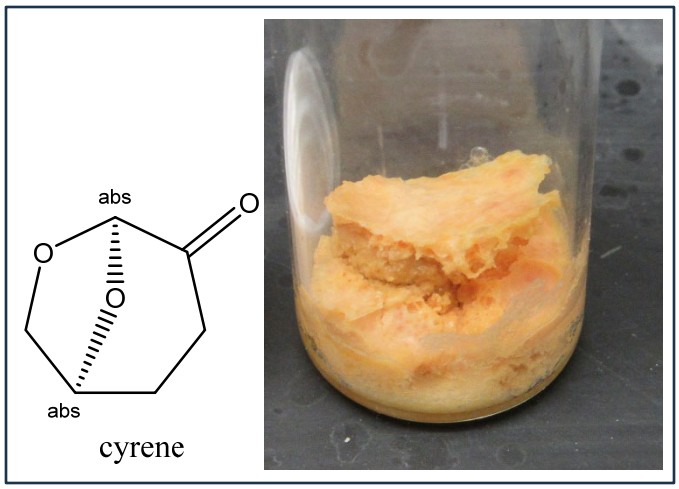

Figure 34. Structure of Cyrene solvent and reaction product of Li_3N, water, and Cyrene.

The conversion of LiOH to Li_2CO_3 may consume lithium ions and alter the equilibrium conditions. Formation of a white insoluble solid has previously (Figure 33) been identified as a mixture of LiOH and Li_2CO_3. The material was subsequently washed and the soluble material was decanted from the insoluble white solid. The soluble fraction was dried and re-analyzed but found to contain the same composition as before (Figure 35). Since Li_2CO_3 is poorly soluble, it was conjectured that the soluble fraction was initially LiOH rich, but as the solution dried and exchanged CO_2 with the atmosphere, the LiOH reacted to form Li_2CO_3. The produced solid could not be subsequently redissovled in water. Formation of a white solid precipitate on Li_3N pellets is thus likely to be Li_2CO_3. Prolonged air exchange with LiOH-containing aqueous solution is likely to sequester Li ions. While this would shift equilibrium conditions to enable the Li_3N pellet to fully react, the poor solubility of Li_2CO_3 is likely to form a shell around the pellet.

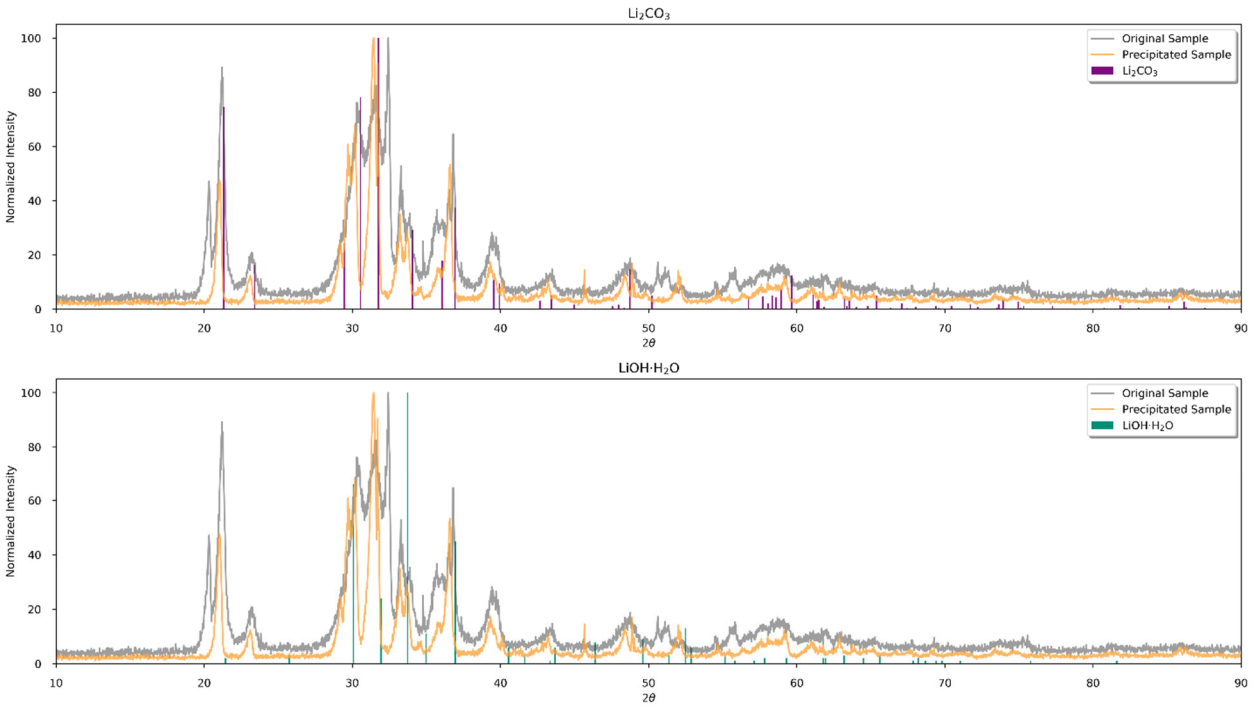

Figure 35. XRD scan of reprecipitated Li_3N decomposition product. The precipitated sample contains Li_2CO_3, which likely formed while drying.

2.1.7 Reaction of Pellets with HD

Reaction studies were also done with HD and the Li_3N pellets F09-153, F09-138C, and F09-135E, which were pellets made at SNL with small amounts of wax as a binder. The pellets did not break up in the HD, and they were still visibly intact. No reaction of HD was observed with $Li_3N + H_2O$ using these pellets, so solubility of wax in HD didn't help to break up the pellets.

Figure 36. 4.0 mL of HD with pellet F09-138C and 0.4 mL H_2O. The intact pellet can be seen at the bottom of the vial.

2.2 Reactions with $LiAlH_4$

Studies were done using lithium aluminum hydride ($LiAlH_4$) as a reagent. $LiAlH_4$ pellets were obtained from Sigma-Aldrich, P/N 323403-100G. This reagent was chosen for study because it is a strong, reactive reducing agent that is commonly used in chemical synthesis, and it is readily commercially available. It has the capability of reducing by contributing 4 electrons, which could potentially decrease the molar ratio of reagent to CA.

The solution ^1H NMR spectrum in Figure 37 shows the beginning reaction in which HD was treated with a small amount of $LiAlH_4$. The $LiAlH_4$ was obtained from a solid pellet, and a small chunk (5 mg) was placed directly on the surface of the neat mustard (400 µL), without use of solvents. Over several hours a physical change was observed, and the mixture appeared to thicken and gel.

The reaction was repeated by adding a $LiAlH_4$ pellet to 5 mL HD in a vial. A small amount of micro bubbling was initially observed. There was no detectable heat or evidence of a strong reaction. When the reaction mixture was sampled, no reaction products were observed. Quantitation of the HD relative to an internal standard showed that 85-90% of the HD that was added was still present even after 49 days of reaction (sample nb0018p65B). We conclude that the HD was not reduced or reacted by the reagent. However, when the vial sat with the cap off, the $LiAlH_4$ reacted probably with water from the atmosphere, and expanded to absorb the HD in a gray or white paste (samples nb097p143B; nb0018p65A, shown in Figure 38; and nb0018p65B). The chunks of $LiAlH_4$ were gone. The brownish color of the original HD faded, indicating that the compound that caused the color was reduced. As a result, the agent was converted into a viscous solid in these conditions, but the toxicity was probably not decreased since there was no apparent reaction with the HD.

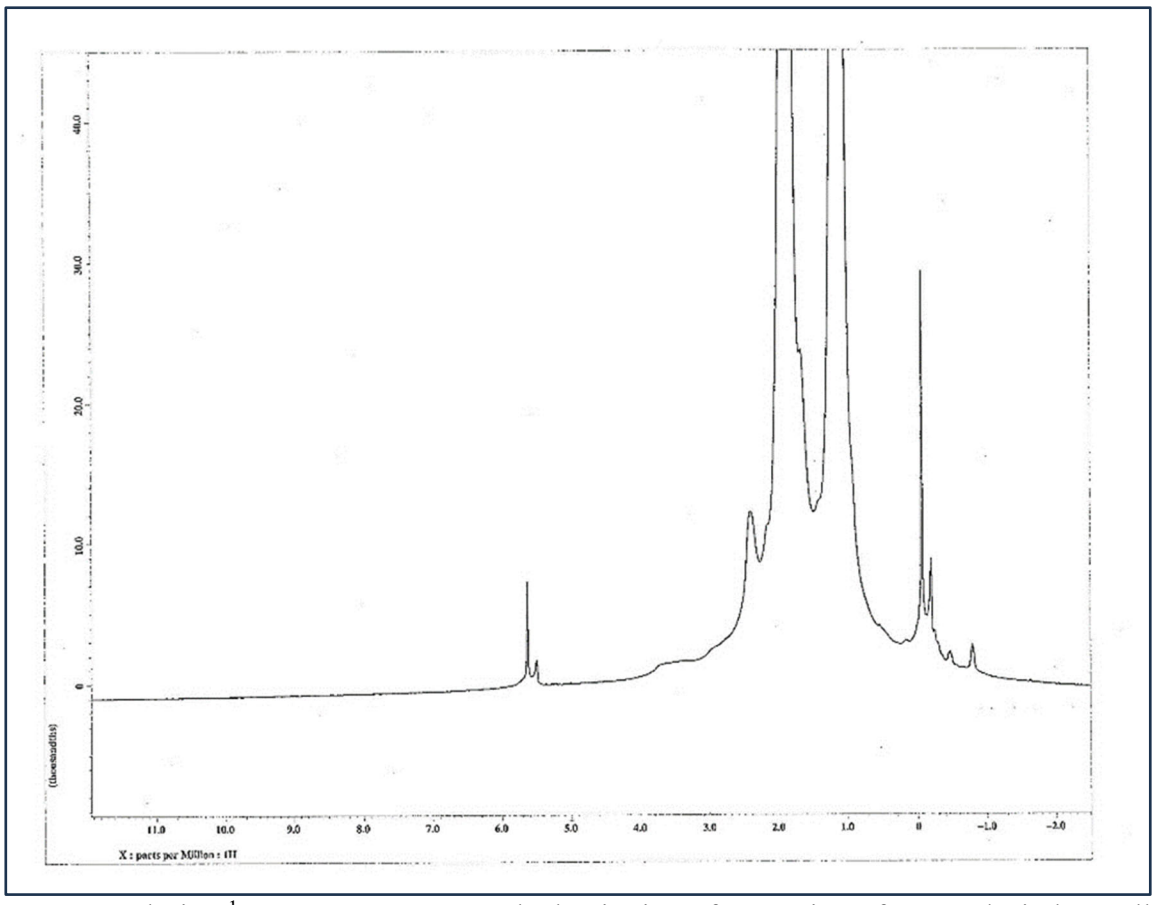

Figure 37. Solution ^{1}H NMR spectrum at the beginning of a reaction of HD and $LiAlH_4$ pellet.

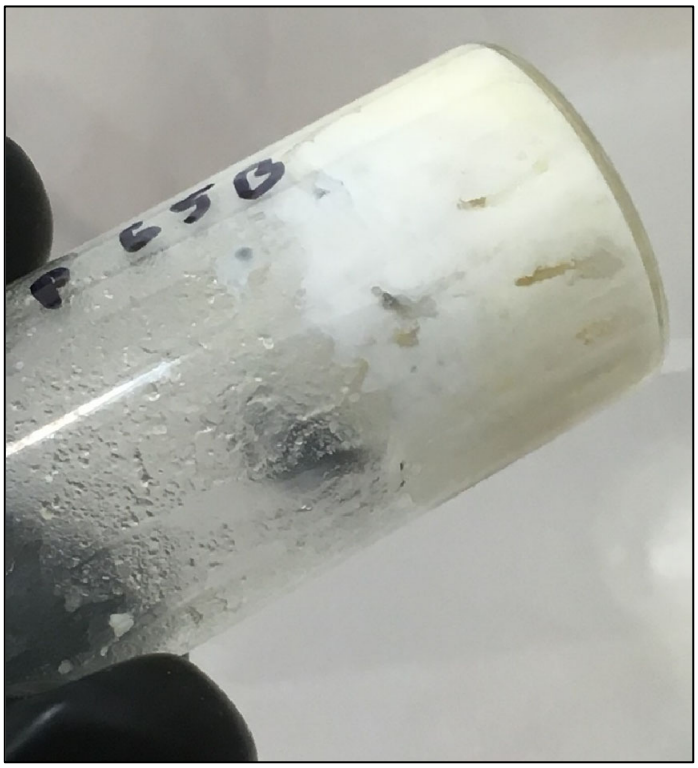

Figure 38. Reaction mixture of HD + $LiAlH_4$, sample nb0018P65B, using 5 mL HD and 0.9 g $LiAlH_4$ (14.5 wt%). After standing for a week uncapped, the reagent expanded to absorb the HD to form a paste.

An HD reaction was done with $LiAlH_4$ that was purchased as a solution in tetrahydrofuran (THF) solution at a 2.0 M concentration (Sample nb097p143A). This solution was miscible with HD, so no solids separated. There was no evidence of reaction, except that the color of the HD faded, shown in Figure 39, and no reaction products were observed in the NMR spectrum.

Figure 39. Reaction mixture of HD + $LiAlH_4$ in THF solution (right, sample nb097P143A), compared to the original HD (left), showing that the reagent removed the color.

2.3 Elimination of HD Using Alkylaluminum Sesquihalide (Friedel-Crafts) Chemistry

The use of a Friedel-Crafts type of reaction strategy appeared promising, since this is a synthesis method that is commonly used for reactions that consume chlorinated compounds. Some results were encouraging, but others didn't show a consumption of the chlorinated HD. In general, the synthesis strategies are developed for making particular products by using chlorinated starting materials, which can be present in molar excess amounts. However, they have not been optimized for consuming all the starting materials as decontamination-type reactions.

Literature studies have indicated that Grignard reactions (also involving organometallic chloride intermediates) are dependent on solvent conditions.[14 15] It is possible that more experimentation on these types of reactions could yield a useful HD decontamination scheme, but it is also possible that the scheme would be so specific to particular solvent and temperature conditions that it wouldn't be reliable under a range of field conditions. A large number of test reactions with simulants were performed to search for reaction conditions.

2.3.1 Synthesis of Alkylaluminium Chlorides from CEES/CEPS

Approximately 300 vial-based reactions were performed at SNL using chloroethyl ethyl sulfide (CEES) and bis-chloroethyl ether (BCEE) as simulants for chemistry of neat HD. After extensive research, a magnesium-based chemistry was developed that demonstrated gelation and neutralization of CEES and BCEE. It was found that magnesium powder and

magnesium-aluminum alloy powder in combination with iodine and tetrahydrofuran initiates a reaction that results in the slow (*hours to days*) solidification of the neat simulant. The addition of copper(II) chloride ($CuCl_2$) enhanced the reaction mostly likely through Kumada coupling.[16]

Visual observations of the magnesium-based reactions on CEES and BCEE repeatedly showed varying degrees of solidification of the neat simulants. The inconsistency of the reactions was attributed to lack of stirring of the reactions resulting in the metal powders falling out of solution. Slow stirring of the reactions to keep the metal powders suspended in solution was key to reproducibility of the reactions. Smaller particle sizes (e.g., 325 mesh) were easier to keep suspending in solution. Using metal chunks instead of powders was not very effective in achieving solidified reactions. The reactions appeared to take place on the metal surface creating a layer of solid material surrounding the metal chunks effectively quenching the reaction. $CuCl_2$ was introduced into the reactions via saturated solutions in THF. Pictures of one milliliter reactions using the magnesium-based chemistry for CEES and BCEE are shown in Figure 40. The reactions circled in green yield highly viscous or solid solutions and were the identified reaction combinations for testing on HD at ECBC.

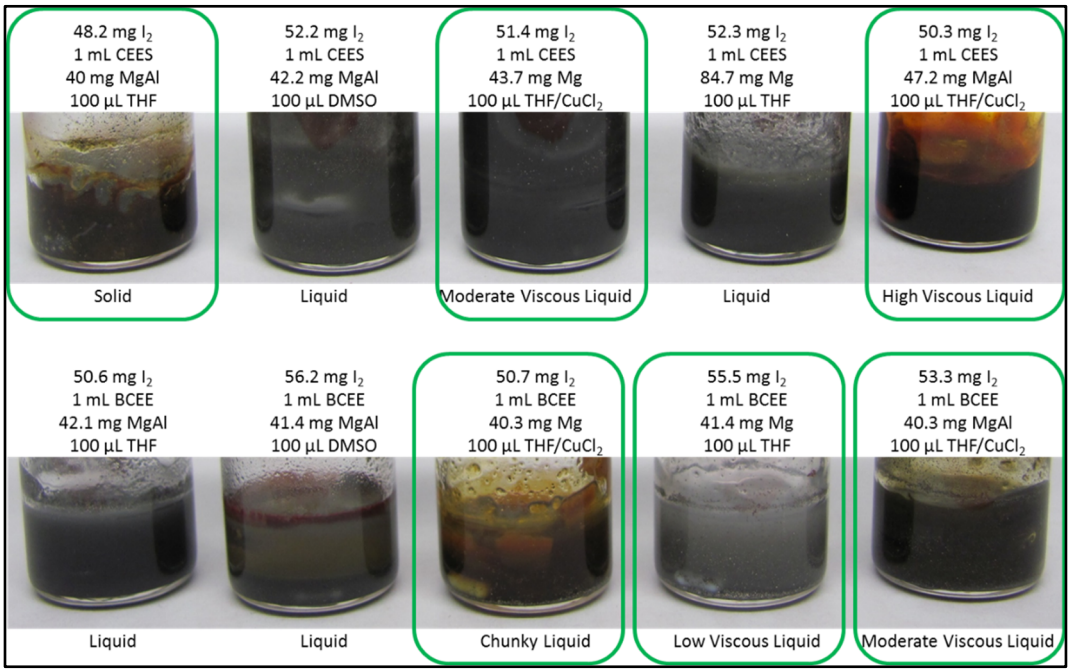

Figure 40. Pictures of reactions of CEES (top row) and BCEE (bottom row).

Selected reactions were analyzed via solid state ^{13}C Magic Angle Spinning (MAS) NMR and are outlined in Table 1. These reactions were slowly stirred and heated (30 °C/86 °F) in order to drive the reaction to near completion for analysis of the reaction products. Figure 41 depicts ^{13}C MAS NMR spectra of the solid reaction products for CEES (top, 044A and 044E) and BCEE (bottom, 044H and 044J).

^{13}C MAS NMR analysis of the solid product formed for the reaction with CEES revealed the disappearance of the chloroethyl group indicative of neutralization of CEES. For the 044A and 044E there is a significant loss of the CEES, most notable is the reduction of the (a') and (b') resonances.

Numerous other carbon species are produced in this reaction, with the observed chemical shift range δ = +45 to + 10 ppm consistent with alcohols, aliphatic species and chlorinated aliphatic chains. Some of these resonances overlap with the remaining CEES. NMR analysis of the solid products formed indicate only the presence of BCEE even though the reactions contained only small amounts of liquid and significant gel/solid material.

For reaction 044H and 044J the only significant carbon species belong to BCEE. Either this is a polymerization with THF to make longer ether species, or the "gel" like properties of the precipitate are not related to a reaction of the BCEE. If it was polymerizing (significantly) the ratio of the ether resonance (a) should increase with respect to the Cl carbon environment (b) from an endgroup analysis. The ratio is approximately 1:1, arguing against extensive polymerization.

Table 1. Outline of Reactions used for NMR Analysis of Solid Reaction Products

RXN ID	**Simulant**	**Corroder**	**Metal**	**Catalyst**
044A	CEES	I_2	MgAl (small)	THF
044E	CEES	I_2	MgAl (small)	THF/$CuCl_2$
044H	BCEE	I_2	Mg	THF/$CuCl_2$
044J	BCEE	I_2	MgAl	THF/$CuCl_2$

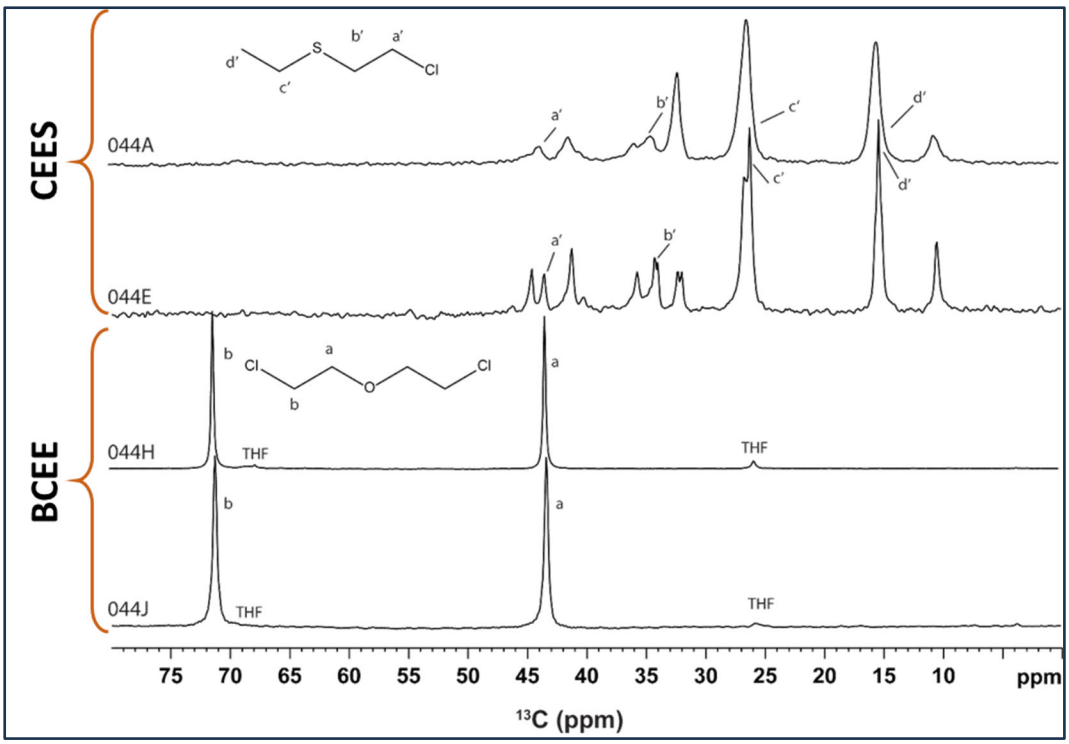

Figure 41. Solid state ^{13}C MAS NMR analysis of solid reaction product.

2.3.2 Synthesis of Alkylaluminium Chlorides from HD

Following the reactions for BCEE and CEES, HD reactions were studied at CBC. A series of reactions based on Friedel-Crafts reactions of neat HD were done using the conditions that are listed in Table 2, following the results in Table 1. The goal was to find a catalytic approach that would consume the HD with a minimal amount of metal and reagents. Mg or Mg/Al alloy were added as solid metal turnings or powder with various catalysts or cosolvents. I_2 was added to all the reaction mixtures to corrode the metal oxide surface to expose the HD to non-oxidized metal.

Table 2. Reaction Information for Magnesium Reactions Analyzed Via ^{13}C NMR in Liquid Sample Tubes

Sample ID	Agent	Metal	Corroder	Catalyst
81A	373 µL HD	14.93 mg MgAl	19.12mg I_2	37 µL THF/$CuCl_2$
81B	393 µL HD	15.57 mg Mg	19.64mg I_2	39.4 µL THF/$CuCl_2$
83A	386 µL HD	16.29 mg Mg	19.28 mg I_2	39 µL THF
83B	200 µL HD	16.07 mg MgAl	21.93 mg I_2	40 µL THF
85A	400 µL HD	15.64 mg MgAl	22.29 mg I_2	40 µL d-DMSO

There were signs of reaction for some of the compositions. Figure 42 shows the NMR tube with sample nb097p85A. A solid mass is formed in the reaction, although there is still liquid HD on top of the solid, and the analysis of the liquid shows that there are no significant reaction products. Inverting the tube multiple times was not sufficient to mix the solid and liquid components.

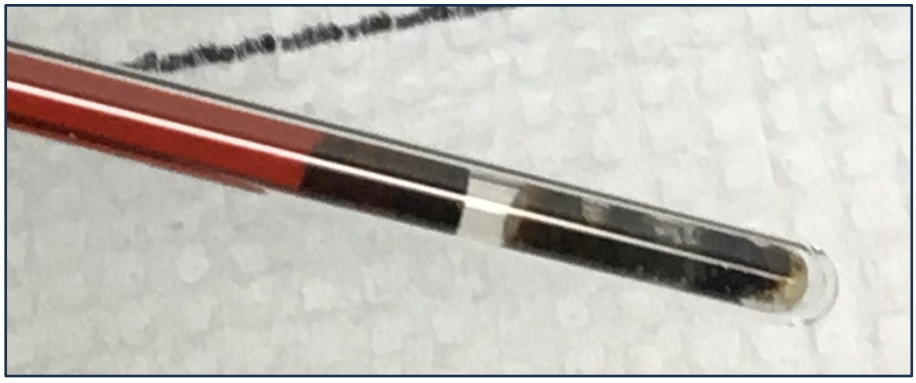

Figure 42. Reaction mixture in NMR tube of HD + MgAl metal + I_2 + DMSO, sample nb097p85A (see Table 2).

Two reaction runs with CEES were done for comparison to simulant results at SNL. Solid residue was also observed, but no reaction products were detected corresponding to the results shown in Figure 41 for CEES. There was no evidence of HD reaction products with the residual HD, shown in the spectrum in Figure 43. The resonances from the unreacted HD were observed at δ = + 43 and +34 ppm, while the THF resonances were observed at δ = +25 and +67 ppm. In 85A, the DMSO-d6 (deuterated) gives a minor multiplet resonance at 39.5 ppm. The relative concentration of these HD carbon species remains essentially unchanged during the reaction, as shown in Figure 43. This suggest that the reaction chemistry does not degrade the HD into new speciation.

Some samples formed a thick plug of porous solid material that increased the viscosity. It was possible that HD was reacting with the metal to form a solid that we couldn't analyze using methods for liquids NMR.

These reactions required more than 10 wt.% of reagents, particularly including I_2, which is dense, heavy, and potentially toxic. This reagent was needed to form the active Mg or Al reagent for the Friedel Crafts reaction, and to transform the metal reagent into a reactive species. Additional solvents and $CuCl_2$ catalyst (saturated solution of solid $CuCl_2$ in THF solvent) were also added to some of the mixtures.

Since a considerable amount of residual HD was observed, it would be necessary to do a toxicity study of the reaction mixtures to determine whether the toxicity has been reduced by the reaction. Due to the expense of this testing, it would be preferable to optimize the reaction so that toxicity studies of only a few of the reaction mixtures are necessary.

Based on the limited success with the sesquahalide chemistry, studies were done with other types of reagents with HD.

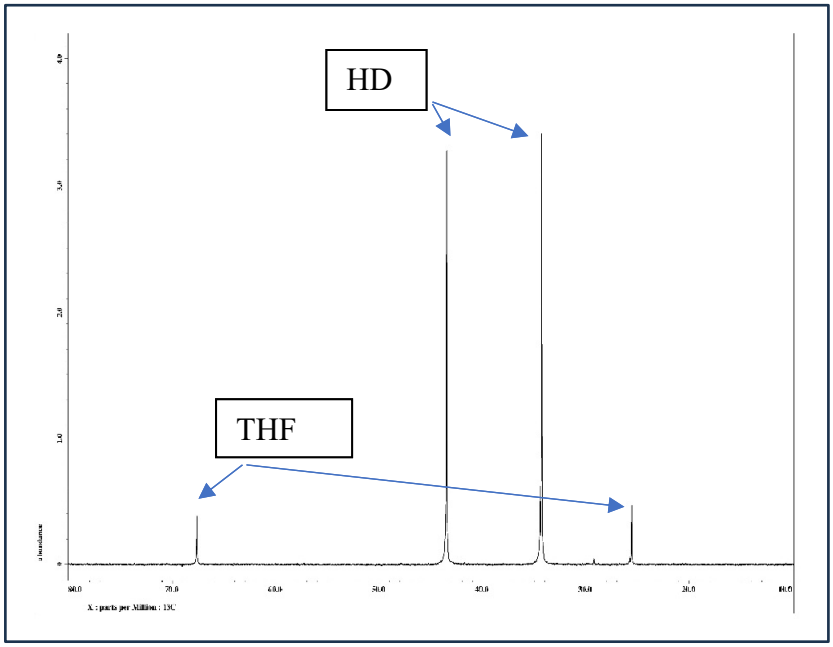

Figure 43. ^{13}C NMR spectra showing no reaction products with HD.

2.4 Other Reactions

Although both $LiAlH_4$ and $Li_3N + H_2O$ met the limited goal of forming a solid reaction product, neither of them were effective at reacting with the HD to decrease the toxicity. As a result, we did a survey of other possible reagents with different ratios, shown in Table 3, some of which were discussed previously.

Almost all of these reagents were surprisingly unreactive. That includes HTH (high test hypochlorite, or $Ca(OCl)_2$ in water), STB (supertropical bleach, or $Ca(OCl)_2$ and NaOH in water), and Na metal. Reaction of HD with Na metal was rapid only when it was heated to 160 °C, above the melting point of the metal.

We hypothesized that the reactions don't occur for most of these reagents because of unfavorable solvent affects in the presence of pure HD. The reactions are expected to proceed by formation of a three-member sulfonium ion intermediate, and this ionic intermediate is not stabilized in the nonpolar solvent.

2.4.1 Reaction of HD with $NaOCH_3$

The most promising reagent was $NaOCH_3$, which showed reaction and formation of a solid residue. A photo of the reaction mass is shown in Figure 44. However, the reaction requires a larger amount of reagent than the target amount, 68% by weight. For 24 wt%, the

amount of residual HD decreased to 55% after 6 days. For 55 wt%, the residual HD decreased to 12% after 6 days.

2.4.2 Reactions of HD in the Presence of Polar Solvents

HD reactions were studied with a polar solvent added. It was hypothesized that the presence of a polar cosolvent may stabilize the sulfonium ion intermediate, which could speed up the reaction. Reactions were started using the solvent propylene carbonate. Reagents were $Li_3N + H_2O$, $NaOCH_3$, HTH ($CaOCl_2$), or $NaMoO_4$. No results from these survey reactions were found that were promising.

Table 3. Reagents Surveys to Look or Reactivity with HD.

Primary Reagent	**Wt. Ratio to HD**	**Secondary Reagent/ Cosolvent**	**Vol. Ratio to HD**	**Sample No.**	**Residual HD percent, days of reaction**
Mg-Al Turning/Powder	4%	THF or $THF/CuCl_2$	8%	NB0018P19C, NB0018P19D	No major reaction prod. after 14 d
HTH solution[a)]	8%			NB0018P75A	90% after 26 d
STB[b)]	8%			NB0018P75C	93% after 28 d
STB[b)]	8%	THF	20%	NB0018P75D	81% after 28 d
$Fe_2(CO)_9$[c)]	10%			NB0018p99A	No reaction prod.
Fe(II) acetate[c)]	10%			NB0018P99C	No reaction prod.
Fe(II) sulfate[c)]	11%			NB0018P99D	No reaction prod.
$NaMoO_4$[d)]	12%			NB0018P99B	No reaction prod.
$NaOCH_3$[e),f)]	35%			NB0018P99E,	30% after 9 d
$NaOCH_3$[e)]	24%	MeOH	10%	NB0018P101B	55% after 6 d
$NaOCH_3$[e)]	55%	MeOH	15%	NB0018P101C	12% after 6 d
Li metal[e)]	7.6%			NB0018P101A	90% after 30 d
Na metal[e)]	7.9%			NB0018P107A	92% after 17 d
Na metal[e)]	7.9%	Heat to 160C		NB0018P107A	71%
$LiBH_4$[e)]	8.3%			NB0018P101D	100% after 2 d
HTH solid	20%	Propylene carbonate	20%	NB0018P123C	48% after 2 months
$NaOCH_3$[e)]	30%	Propylene carbonate	20%	NB0018P123B	30% after 2 months
Li metal in ethylene diamine	10%			NB0018P139B	90% after 1 month

a. $Ca(OCl)_2$ in water.
b. Supertropical bleach, $Ca(OCl)_2$ and NaOH in water.
c. Fe(II) compounds were added to attempt to form HD Heel, a solid found in many stored ton containers of HD.
d. Possible oxidizer.
e. Possible reducing agent.
f. Reagent was added incrementally over several days to a total of 35%.

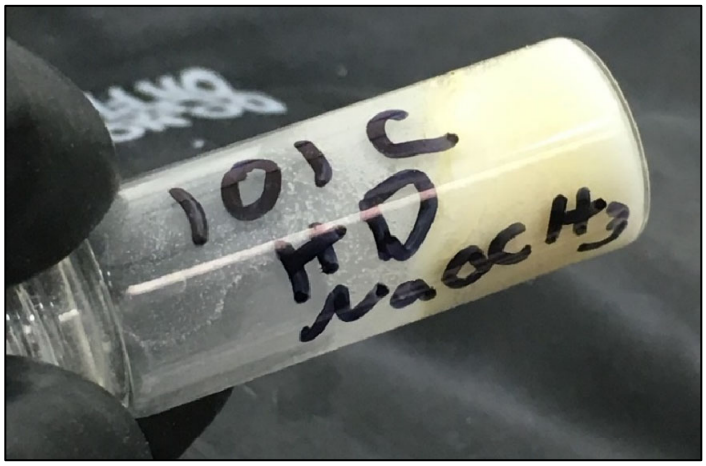

Figure 44. Reaction mixture of HD with $NaOCH_3$, 55 wt% ratio. The photo was taken after 2 days of reaction time, and there was still 88% residual HD. After 6 days of reaction time, the residual HD was 12%.

2.4.3 Reactions of HD with Ti Compounds

Another small-scale reaction study of HD was done with the organometallic reagent tetrakis(dimethylamido) titanium (IV), $[(CH_3)_2N]_4Ti$. Transition metals like Ti are higher molecular weight than the previous reagents that we have studied, but Ti has the advantage of being tetravalent and it is well known to form a variety of solid materials. Using a mixture with 20% by volume (15% by weight to HD) of the Ti compound with HD and no water, a solid formed after two weeks and continued to become harder in 5 weeks, shown in

Figure 45. The reagent reacts vigorously with water, so water wasn't added. Most of the HD was found to be present, and there were no indications of reaction products by using a quantitative ^{13}C NMR analysis.

Even though this reagent didn't destroy HD, it may be worth pursuing this reagent or other similar reagents to look for one that reacts with HD. Similar tetravalent compounds can be purchased with hafnium and zirconium as well as titanium compounds such as $Ti(OCH_3)_4$.

Figure 45. Reaction of HD with $[(CH_3)_2N]_4Ti$, sample NB0049P17A after two weeks of reaction time.

2.4.4 Reactions of HD for Polymerization

A study was done by Patrick Riley and co-workers to find a reaction of HD with bisphenol A that could lead to a polymerization chain reaction between the two chloroethyl groups of HD and two deprotonated phenol groups of bisphenol A.[17] The project had promising results. A reaction of CEES with phenol in the presence of caustic and water went to completion to substitute a phenoxy group for chloride to eliminate the chlorine-carbon bond.

The reaction of HD with phenol or bisphenol A in the presence of caustic and water reacted partially to substitute with chlorine-carbon bonds, although it didn't go to completion. It is possible only 1 of the 2 C-Cl groups reacted. A viscous liquid was formed that may have been polymer or a higher-molecular-weight product. Because C-Cl bonds were left, the product could still have vesicant properties, but toxicology studies were not done to determine how toxic the product was. The ratios of reagents were not minimized to meet the goals of this project, so additional work is required to determine the minimal amounts of reagents to produce a reaction.

Another study was done with several epoxy compounds to determine if they would polymerize with HD. The four epoxy compounds were shown in Table 4. All four compounds were purchased from Sigma Aldrich (MilliporeSigma, St. Louis, MO).

Table 4. Four Epoxy (diglycidyl or triglycidyl ether) Compounds Studied for Reaction with HD

Bisphenol A diglycidyl ether	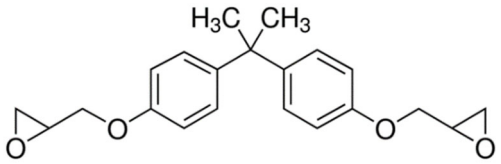
Resorcinol diglycidyl ether	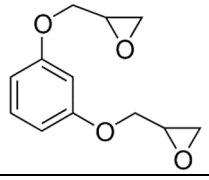
Trimethylolpropane triglycidyl ether	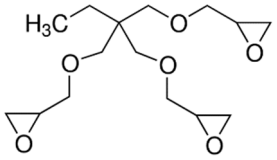
N,N-Diglycidyl-4-glycidyloxyaniline	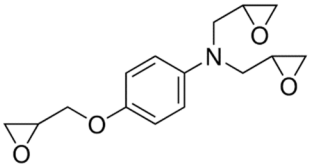

An experiment was done to mix HD with each epoxy compound with a ratio of 70-100 wt% of epoxy to HD. There was no sign of reaction after 24 h. Then about 10% ethylene diamine was added as a hardener. In 4 days or less, the 4 mixtures hardened to about the same extent. However, all 4 mixtures contained a significant amount of HD that didn't appear to react and that could be extracted from the solid epoxy using chloroform as a solvent and swelling agent. The extracts were analyzed by proton NMR spectroscopy.

The reaction of bisphenol A required caustic to deprotonate the reagent before reaction with HD, and it reacted better in the presence of water. This implies that ionic intermediates like a three-member-ring sulfonium ion or else ionic products like chloride are involved in the reaction, and they are dissolved in aqueous solution. For the epoxy reactions, the nonpolar epoxy compound may mix with the HD more effectively, but a radical or non-ionic reaction mechanism apparently doesn't cause a reaction to displace chlorine.

3. AB INITIO MODELING

3.1 HD Reaction Mechanisms and Energetics with Amines

Ab initio molecular dynamics (AIMD) simulation was used as a "gold standard" to benchmark classical force field molecular dynamics (FFMD) for modeling local structures of CAs and simulants. Radial distribution functions (RDFs) were used to investigate the molecular liquid structures of these compounds and to compare the FFMD structure with AIMD. Details

about the computational methods are described in other publications.[18] [19] The Gaussian 09 software was used without additional modification. All structures were geometry optimized (atomic coordinates and electronic structure). Calculations were performed using Sandia's high performance computing facility. Tens of thousands of core-hours of computer time were used in the study.

A goal of this study is to assist experimental studies with insight into the formation of the intermediates and products in the reaction of HD with different kinds of amines, specifically ammonia, ethylamine, and diethylamine. To explore the energetics and make comparisons of the reaction pathway intermediates and transition states, we investigated two reaction pathways, S_N2 and E2, shown in

Figure 46.

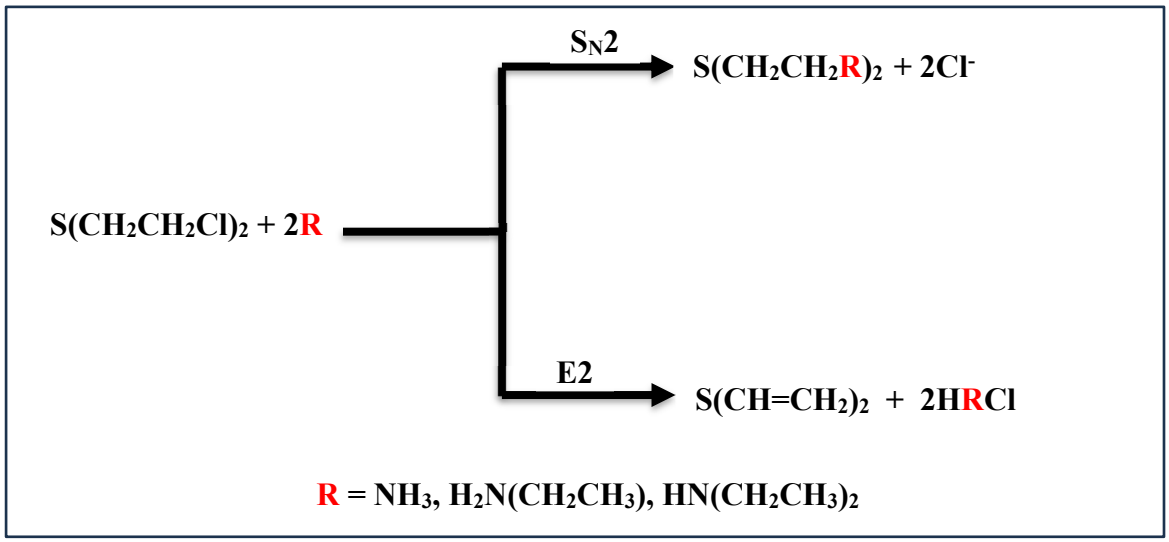

Figure 46. Generalized pathways of S_N2 and E2 for reaction of sulfur mustard with amines.

Calculated reaction energies for HD and BCEE (Figure 47) with various amines were studied to provide theoretical insight to the spontaneity of the reactions. We explored HD pathways of S_N2 and E2 elimination reactions (Figure 48 and Figure 49). Each reaction requires two intermediates and two transition states to form their theoretical products. The S_N2 reaction undergoes two sequential displacement steps that involve the substitution of each chlorine atom with an amine to form either a primary, secondary, or tertiary product (Figure 48 shows tertiary). On the contrary, HD can go through an E2 elimination pathway that involves a sequential twofold hydrogen abstraction that includes the formation of a carbon-carbon pi-bond that kicks off chlorine atoms to form the twofold unsaturated product (Figure 49). Calculated free energies are shown in Table 5.

Table 5. Transition States, Intermediates, and Product Free Energy Values (kcal/mol) Relative To Reactants Along E2 and S_N2 Reaction Pathways.*

Dielectric 78 E2/S_N2	TS1	IM1	TS2	Product
HD + NH_3	26.19/24.63	-19.10/-12.63	14.96/17.22	-33.28/-20.61
BCEE + NH_3	31.01/27.22	-15.13/-7.98	15.56/21.40	-30.84/-16.66
HD + $H_2NCH_2CH_3$	23.62/22.17	-18.92/-15.16	10.83/12.45	-33.09/-25.74
BCEE + $H_2NCH_2CH_3$	25.59/27.88	-18.35/-13.15	10.83/14.07	-37.27-25.24
HD + $HN(CH_2CH_3)_2$	22.92/20.79	-25.20/-23.40	3.94/20.73	-45.64/-39.92
BCEE + $HN(CH_2CH_3)_2$	25.88/27.99	-23.40/-13.80	10.40/31.40	-43.14/-25.84
Dielectric 3.6 E2/S_N2				
BCEE + $HN(CH_2CH_3)_2$	34.05/35.22	-2.90/-14.41	29.33/24.84	-4.09/-26.24

Dielectric refers to the dielectric constant used to represent the solvent (continuum model). A dielectric constant of 78 corresponds to water, 3.6 corresponds to diethylamine.

Given the pathways, (Figure 48 and Figure 49) we explored the free-energy difference (relative to reactants) along the reaction paths with each amine in different solvent environments (water and diethylamine). The relative energies for E2 and S_N2 reaction pathways of HD in water (dielectric constant 78) are shown in Figure 50.

Starting from the reactants to the first transition state (TS1), we immediately noticed significant energy barriers among the E2 and S_N2 reactions between the different amines: TS1 energies are between 22.92 to 26.19 kcal/mol for E2, and 20.79 to 27.99 kcal/mol for S_N2. Diethylamine ($HN(CH_2CH_3)_2$) resulted in the lowest energy barrier for E2, while ethylamine ($H_2NCH_2CH_3$) resulted in the lowest barrier for S_N2.

After crossing TS1, the reactions fall into a local minimum as an intermediate (IM1), then to the final product via the second transition state (TS2). The S_N2 reaction results in the addition of the amine from the substitution of a chlorine atom. (Figure 48). E2 results in the double bond formation from the first abstraction of a hydrogen (Figure 49). For both E2 and S_N2, $HN(CH_2CH_3)_2$ exhibits the lowest free-energy, -21.28 kcal/mol and -23.40 kcal/mol, respectively. TS2 shows a relatively lower energy barrier for diethylamine along the E2 pathway (3.94 kcal/mol), while a larger barrier exists for the S_N2 pathway (20.73 kcal/mol).

After crossing TS2, the reaction falls into a global minimum for both S_N2 and E2 reactions. Overall, the E2 pathway exhibits the lowest free energy for the formation of the unsubstituted product that ranges between -45.64 to -33.09 kcal/mol. The formation of the tertiary amine exhibits the most stable reaction among the amines. However, the high initial energy barrier required for any of these reactions suggests very slow rates at room temperature.

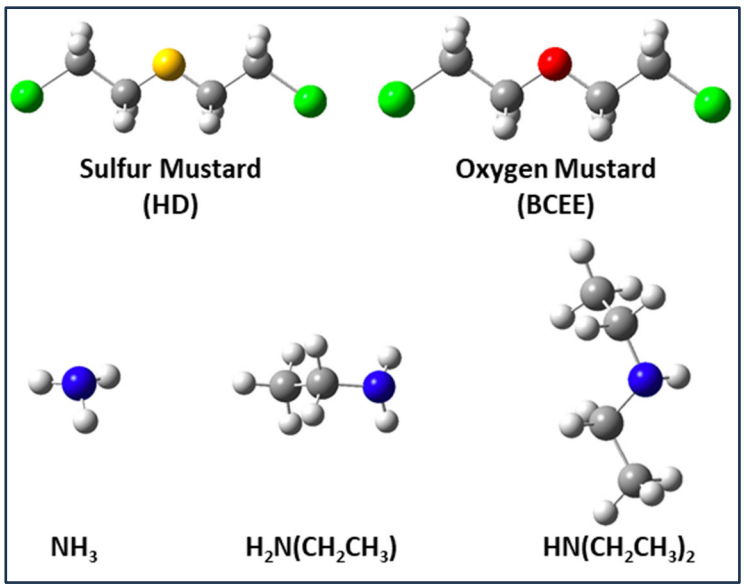

Figure 47. Snapshots of optimized electronic structures of sulfur mustard (HD), simulant BCEE, ammonia (NH_3), ethylamine ($H_2NCH_2CH_3$), and diethylamine ($HN(CH_2CH_3)_2$).

Likewise, we explored the BCEE reaction pathways in water (dielectric constant 78), see Figure 51. Like HD, BCEE follows a similar trend with few differences among the energy barriers and intermediate states.

Along the S_N2 pathway, the different amines experience TS1 energy barriers between 27.22 and 27.99 kcal/mol, while E2 has TS1 barriers between 29.59 and 31.01 kcal/mol. The elimination of the first hydrogen has the largest TS1 (31.01 kcal/mol) for NH_3, while $HN(CH_2CH_3)_2$ has the largest TS1 barrier for S_N2. Upon crossing E2 and S_N2 TS1, a first intermediate (IM1) is achieved. The S_N2 has minimum free energy between -13.85 to -7.98 kcal/mol with $HN(CH_2CH_3)_2$ forming the most stable intermediate.

The first carbon-carbon double bond is formed more favorably with diethylamine, but only slightly lower than ethylamine (-13.15 kcal/mol). Additionally, the formation of IM1 (first double bond formation) is more stable with diethylamine. To move from the first minimum to the second transition state (TS2), energy barriers of 14.07 to 31.40 kcal/mol exist along the S_N2 pathway, with ethylamine having the lowest barrier and diethylamine having the largest. However, the E2 pathway exhibits larger barriers ranging between 10.40 to 15.45 kcal/mol, with diethylamine having the lowest barrier.

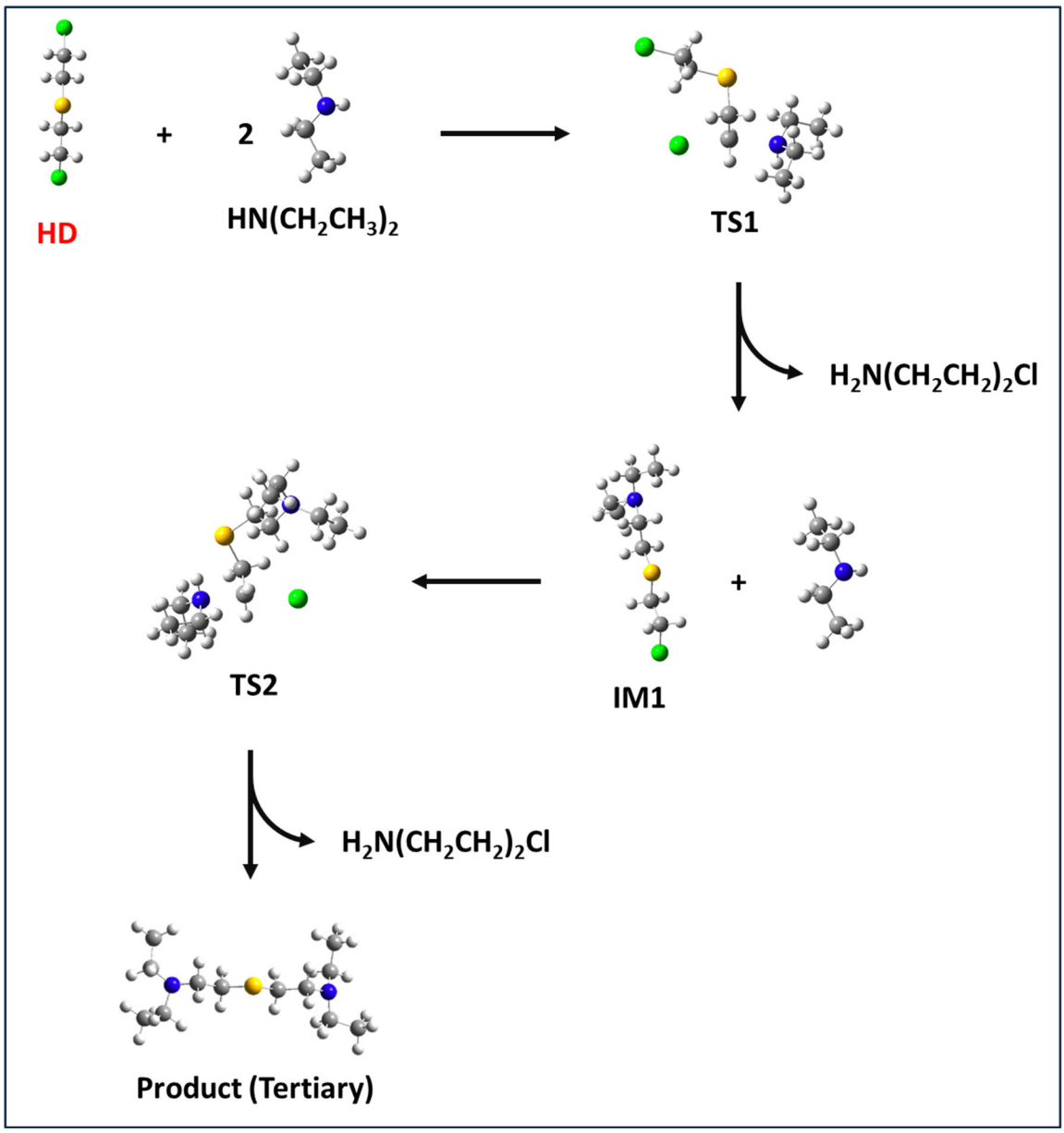

Figure 48. S_N2 reaction pathway of sulfur mustard.

After TS2, the reaction proceeds to formation of the twofold substituted amine product (similar to Figure 49) with twofold substituted tertiary amine having the lowest energy and primary amine with the greater free energy. It should be noted that in all cases diethylamine forms the most stable intermediates and products along both pathways.

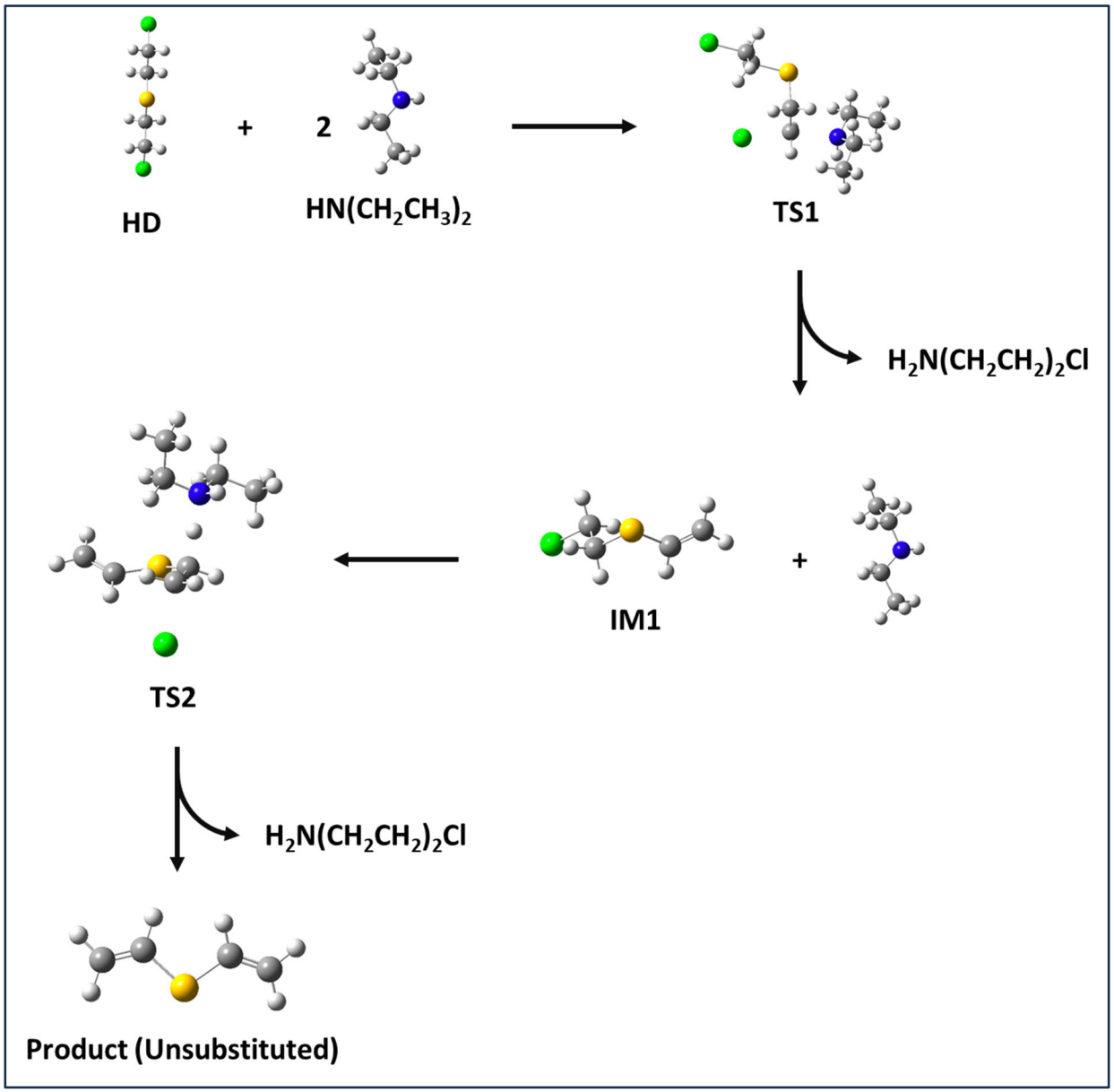

Figure 49. E2 reaction pathway of sulfur mustard.

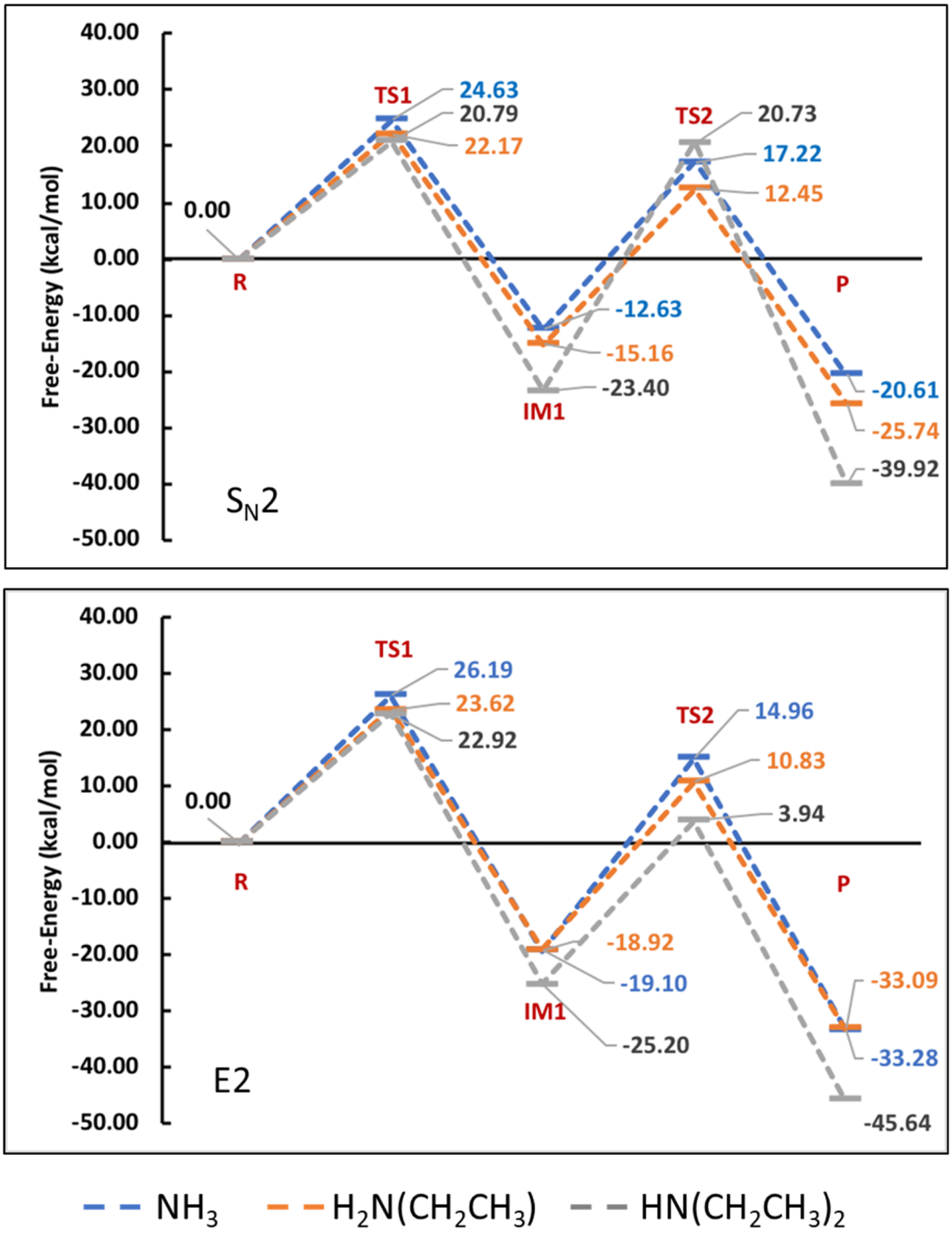

Figure 50. E2 and S_N2 reaction pathways for the decontamination of HD with different amines [NH_3, $H_2N(CH_2CH_3)$, and $HN(CH_2CH_3)_2$] in dielectric of 78.

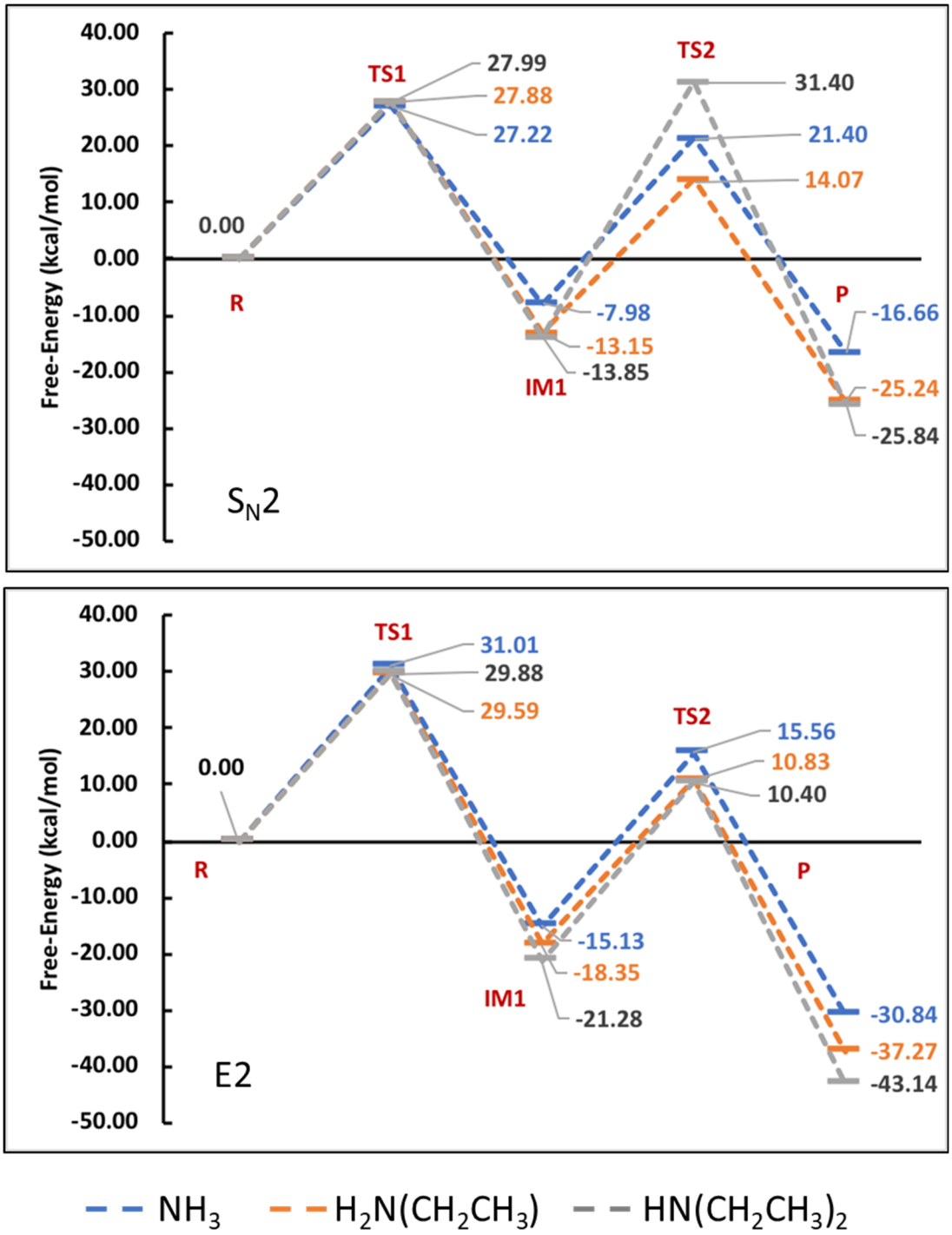

Figure 51. E2 and S_N2 reaction pathways for the decontamination of BCEE with different amines [NH_3, $H_2N(CH_2CH_3)$, and $HN(CH_2CH_3)_2$] in dielectric of 78.

Additionally, we explored the E2 and S_N2 pathways of BCEE with $HN(CH_2CH_3)_2$ in a dielectric of 3.6 (dielectric of $HN(CH_2CH_3)_2$), see Figure 52. In general, E2 exhibits the most favorable pathway, while S_N2 is less favorable. For both pathways, the TS1 energy barrier decreases as the solvent dielectric medium increases (*i.e.*, lower TS2 barrier in water compared to diethylamine). For the S_N2 reaction pathway, the products are only slightly favored thermodynamically (-4.09 kcal/mol).

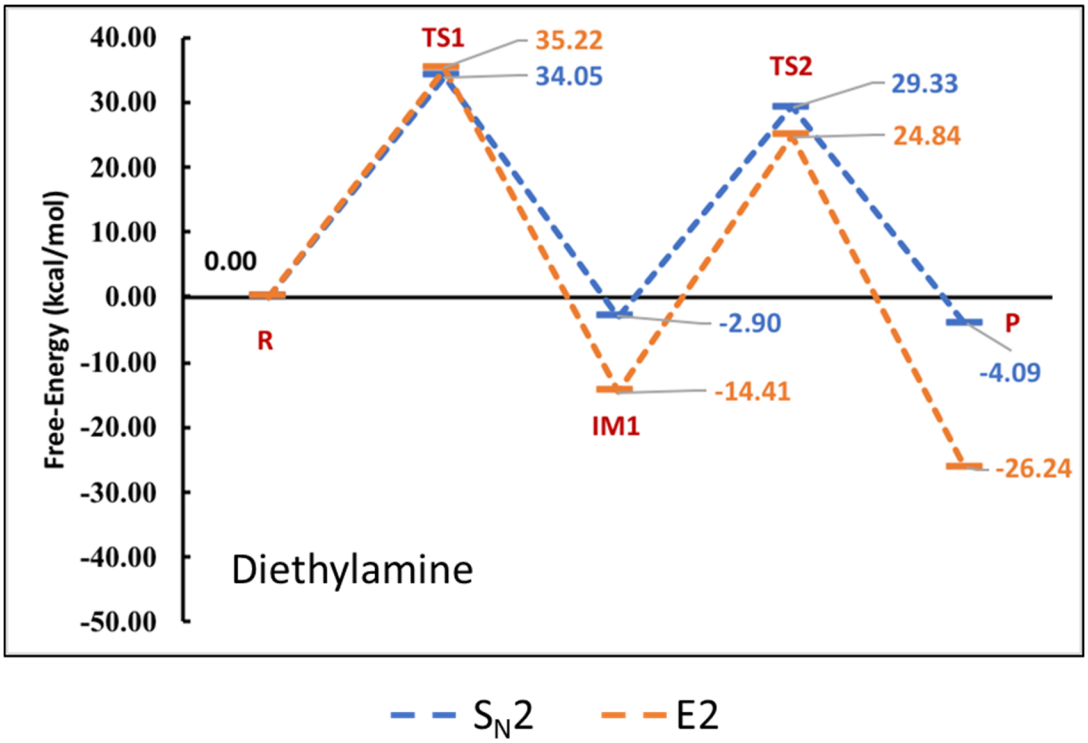

Figure 52. E2 and S_N2 reaction pathway for the decontamination of BCEE with $HN(CH_2CH_3)_2$ in dielectric set to mimic diethylamine (3.6).

3.2 CEES Reaction Mechanisms Through Cyclic Sulfonium Ion

We also investigated the HD simulant CEES, reacting with different classifications of amines. Including ammonia (NH_3), primary $(CH_2CH_2)NH_2$, secondary, and tertiary. Since experimental work has been conducted on CEES with triethyl amine, we complemented those studies. We believe the sulfonium cationic ring is not exclusive to hydrolysis and, therefore, began modeling the reactions with the sulfonium cation to explore the chemical alacrity of the reactions with the different classification of amines and the sulfonium ion, shown in Figure 53.

Figure 53 shows the intermediate formed for each species contains an overall positive charge. Furthermore, most of the intermediates not only contain positive charge, but also contain a hydrogen that can promote further reactions to the neutral product. However, the

reaction of sulfonium ion + triethyl amine ($(CH_2CH_2)_3N$ product lacks the necessary hydrogen for pushing the reaction further and suggests the reaction completes after the first step.

The first step is a simple addition of a specific amine to the sulfonium cation. Table 6 shows the free energy accompanied with the addition of each amine sulfonium cation. Although all the reactions undergo the addition spontaneously, NH_3 shows to be the least favorable reaction, while the $(CH_2CH_2)_2NH$ adds to the sulfonium most favorably.

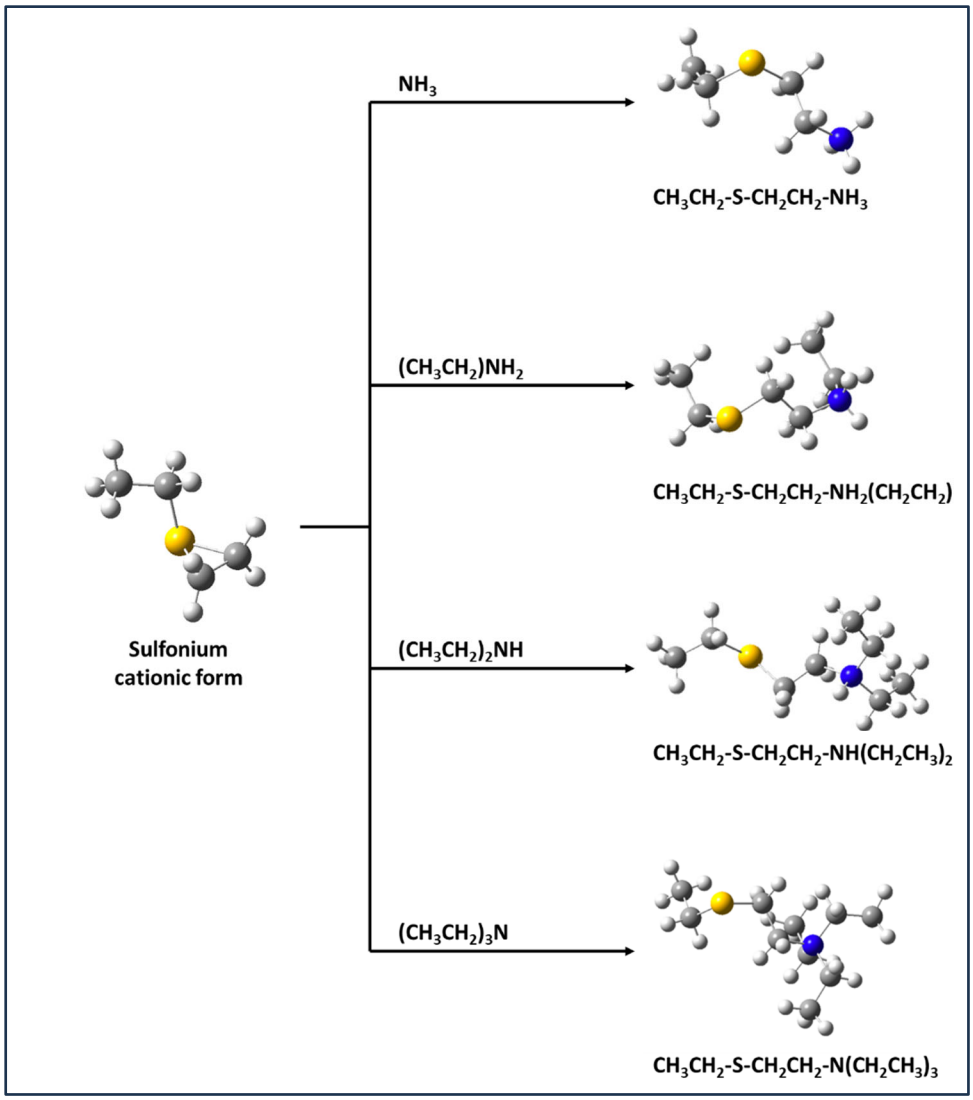

Figure 53. Reactions of CEES with different classifications of amines starting from the sulfonium ring.

Table 6. Gas Phase Free Energies for CEES Reaction with Different Classification of Amines.

Reactants			Products	ΔG (kcal/mol)
$[CEES –Sulf]^+$	+ NH_3	=	$[CH_3CH_2\text{-}S\text{-}CH_2CH_2\text{-}NH_3]^+$	-10.41
$[CEES –Sulf]^+$	+ $(CH_3CH_2)NH_2$	=	$[CH_3CH_2\text{-}S\text{-}CH_2CH_2\text{-}NH_2CH_2CH_3]^+$	-17.81
$[CEES –Sulf]^+$	+ $(CH_3CH_2)_2NH$	=	$[CH_3CH_2\text{-}S\text{-}CH_2CH_2\text{-}NH(CH_2CH_3)_2]^+$	-66.06
$[CEES –Sulf]^+$	+ $(CH_3CH_2)_3N$	=	$[CH_3CH_2\text{-}S\text{-}CH_2CH_2\text{-}N(CH_2CH_3)_3]^+$	-52.71

From our calculations, the most likely event for the reaction to progress forward to the neutral product is from the deprotonation of N-H by a chloride ion (Cl^-). Figure 54 shows the neutral products formed after the deprotonation of the amine hydrogen. Table 7 shows gas phase free energy for the spontaneous formation of the neutral products from deprotonation of the N-H from a Cl^-. The calculated free energies convey that, although NH_3 proceeds least favorably in the first addition step, it readily gives up a hydrogen more freely than the other intermediates.

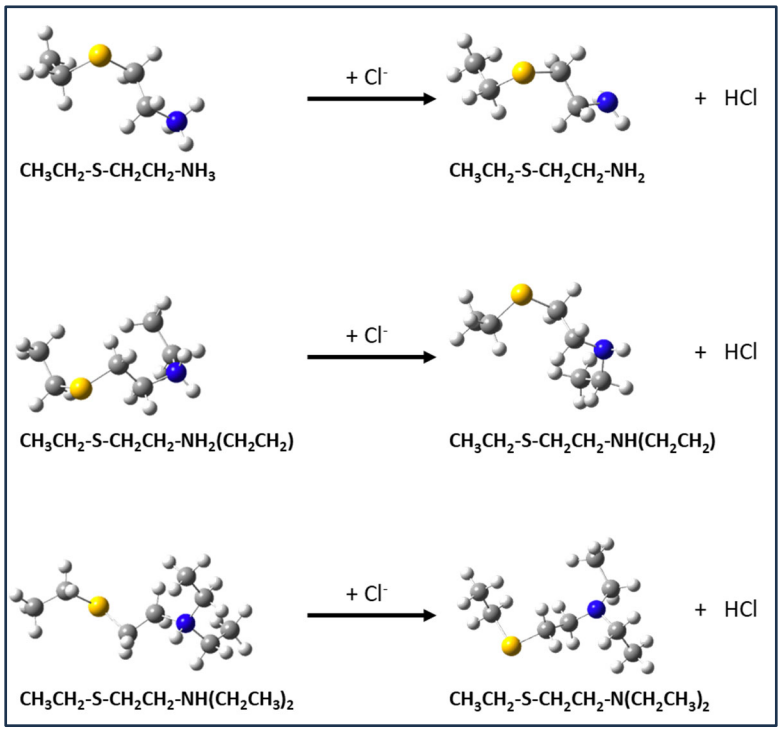

Figure 54. Formation of the neutral products from the deprotonation of N-H.

Table 7. Show the Second Step for the Formation of the Neutral Product.

Reactants				Products			ΔG (kcal/mol)
$[CH_3CH_2\text{-}S\text{-}CH_2CH_2\text{-}NH_3]^+$	+	Cl^-	=	$[CH_3CH_2\text{-}S\text{-}CH_2CH_2\text{-}NH_2]$	+	HCl	-112.64
$[CH_3CH_2\text{-}S\text{-}CH_2CH_2\text{-}NH_2CH_2CH_3]^+$	+	Cl^-	=	$[CH_3CH_2\text{-}S\text{-}CH_2CH_2\text{-}NHCH_2CH_3]$	+	HCl	-104.67
$[CH_3CH_2\text{-}S\text{-}CH_2CH_2\text{-}NH(CH_2CH_3)_2]^+$	+	Cl^-	=	$[CH_3CH_2\text{-}S\text{-}CH_2CH_2\text{-}N(CH_2CH_3)_2]$	+	HCl	-55.87
$[CH_3CH_2\text{-}S\text{-}CH_2CH_2\text{-}N(CH_2CH_3)_3]^+$	+	Cl^-	=	$[CH_3CH_2\text{-}S\text{-}CH_2CH_2\text{-}N(CH_2CH_3)_3]^+Cl^-$		-	

To gain insight into the sulfonium/chloride ion interaction stability due to polarity influence, the ion-pair was studied by investigating the sulfur-chloride (S-Cl^-) distance interactions as a function of dielectric constant (Figure 55). Each calculation began with the same initial configuration similar to Structure 1 in

Figure 56. At low dielectric or gas phase environment, Cl^- attacks the sulfonium ring at the terminal carbon to form a covalent bond, resulting in a linear sulfur mustard. As the dielectric increases, the ion pair between the S/Cl pair become stable. However, as the dielectric increases further, the interaction distance increases, which suggests the sulfonium ion short range interaction begins to weaken. This result is interesting because without explicit water, the short-range interactions are influenced by the dielectric. One can imagine when water is added to the system, the ion-dipole interaction of Cl- and water will play a role. Additionally, it would be interesting to see how aprotic vs. protic solvents influence the S/Cl stability.

To explore the mode of interaction of the Cl^- anion around the sulfonium cation, Cl^- is placed along the CH_2-CH_2 bond by the ring and around the sulfur atom (Figure 55). The structures underwent a geometry optimization to obtain an optimal lowest energy configuration. The most stable sulfonium/Cl^- ion pair interaction is along the sulfonium ring, while the Cl^- positioned aside the sulfur atom yielded second lowest energy, and the Cl^- positioned directly behind the structure interacting with the sulfur atom yielded in the highest mode of interaction. Cl^- seems to be stable in the Structure 1, but more work by charge distribution on the sulfonium ion need to be done along with Natural Bond Orbital (NBO) analysis to provide more support to the analysis.

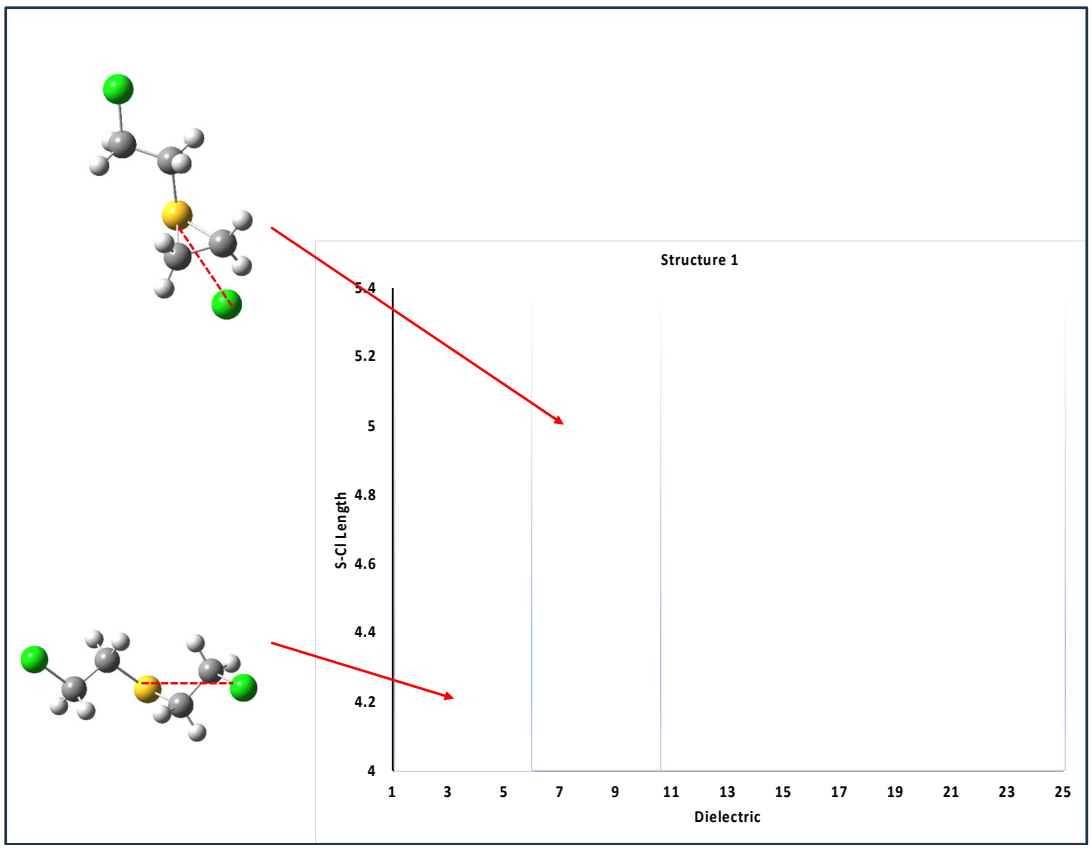

Figure 55. Sulfur/Cl ion interaction distance change as a function of dielectric.

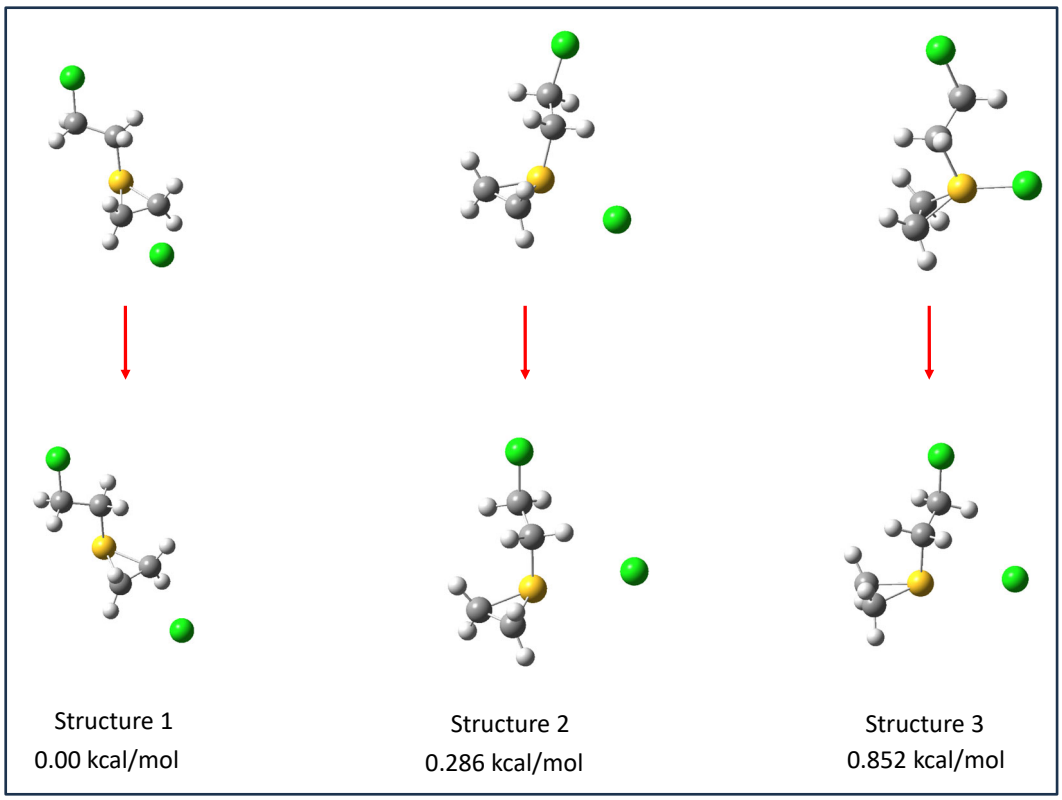

Figure 56. Electronic structure optimization for the sulfonium/Cl ion modes of interaction.

3.3 Machine Learning Methods for Reaction Energetics for Amino Acids

Finally, we explored alternative methods to predict chemical reactions using machine learning (ML) methods. We pursued ML with the short-term goal of predicting physical properties of common agents and simulants, and a long-term goal of predicting chemical reactions.

ML models typically require inputs to be of a fixed dimension. Therefore, the first step involves processing the data to extract useful molecular information from chemical structures while transforming them into a fixed dimensional representation. We did this by transforming molecular formulae into extended connectivity fingerprints (ECFP) in the python module RDKIT.[20 21] These ECFPs are fixed length vectors that capture relevant molecular features and substructures using only a simplified molecular-input line-entry system (SMILES) string.[22] These molecular fingerprints can be used as input to the ML model by themselves, when no additional information is available, or they can be combined with additional features for optimal performance.

A proof-of-concept deep artificial neural network model was constructed to predict solubility using the open-source ESOL aqueous solubility database.[23] This database contains over 1000 chemical compounds with experimental solubility values and five relevant features for each chemical compound (polar surface area, number of hydrogen bond donors, number of rings, molecular weight, and number of rotatable bonds). Additionally, the database

comes with ESOL solubility predictions which are computed from a linear regression model based on the features listed above.

We made three versions of the model, each trained on different input features. The models were trained using 1) only the ECFP, 2) the five expert chosen features, or 3) a combination of the features and the ECFP. The original ESOL model has a mean squared error of 0.83, while our models have mean squared errors of 1.01, 0.67, and 0.47, respectively. This shows that artificial neural networks can achieve high accuracy on property prediction when trained on well selected features combined with ECFPs. Moreover, even without expert chosen features available, the model can make good predictions based on the fingerprints alone.

The predicted values from our combined fingerprint and features model is plotted against experimental values in

Figure 57a. Green and red points corresponding to data that was used to train and test the model, respectively.

Figure 57b shows the performance of our models and the original ESOL model in mean squared error.

There have been numerous published works using artificial neural networks (ANNs) to predict reaction enthalpies; however, many of these methods take optimized geometries as a descriptor (i.e. input to the ANN). Optimized geometries need to be obtained using DFT and, therefore, such methods provide no clear benefit as opposed to using DFT to directly calculate the reaction enthalpy.

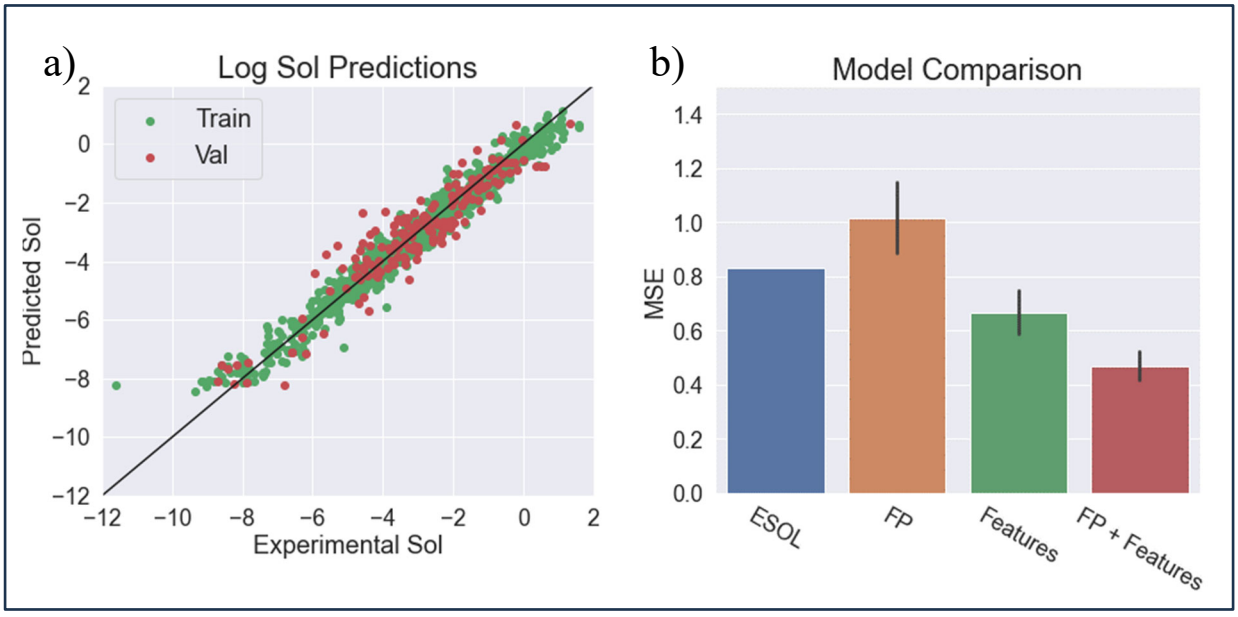

Figure 57. a) Predicted solubility of our fingerprint and features model vs. the experimental values. The black line represents perfect agreement. b) The accuracy of the ESOL model and our models in mean squared error.

We have identified an ANN model, BAND NN, that can perform its own ML-based geometry optimization and does not need DFT optimized geometries to make reaction enthalpy predictions.[24] BAND NN was trained on DFT total energy calculations on theoretical molecules containing elements H, C, N, and O. As such, BAND NN can only be used on molecules made up of these elements and of a limited size (≈10 heavy atoms per molecule). Due to this limitation, BAND NN cannot be used to calculate reaction enthalpies for CA reactions.

We identified another ANN model, TorchANI,[25] that has numerous advantages over BAND NN. Like BAND NN, TorchANI accepts non-optimized molecular geometries and returns optimized structures and thermochemistry information; however, rather than simply providing reaction energies, TorchANI provides reaction energies, enthalpies, and Gibb's free energies. The addition of Gibb's free energy values will more accurately predict reaction favorability compared with reaction energy values alone. Moreover, TorchANI works for molecules containing elements H, C, N, O, Cl, F, and S. This expanded element compatibility allows for prediction of mustard compounds that was not previously possible with BAND NN. Finally, TorchANI provides thermochemistry values more accurately and consistently than BAND NN.

When compared to our DFT standard method (□B97X) for select organic molecules (amino acids and their derivatives chosen for their elemental compatibility with BAND NN), TorchANI and BAND NN have an average error of ≈1.3 kcal/mol and ≈2.3 kcal/mol, respectively. Figure 58 shows the net reaction energy for 13 amino acids to keto acid reactions predicted by BAND NN (blue), TorchANI (green), and AM1 (red), a semi-empirical method similar to the ANNs in computational time, compared to the DFT target value (orange).

Not only is TorchANI often the closest prediction to DFT out of the three methods, but it also did not make any predictions that had a large error (>3 kcal/mol). On the contrary, BAND NN and AM1 both have predictions that had errors in excess of 3 kcal/mol (Thr, Val, Ile for BAND NN and numerous for AM1). Although BAND NN has a low average error, the appearance of these larger inaccurate predictions makes it difficult to trust going forward. However, the ≈1.3 kcal/mol average error, and consistency, for TorchANI is extremely promising and shows that TorchANI predictions are near DFT accuracy.

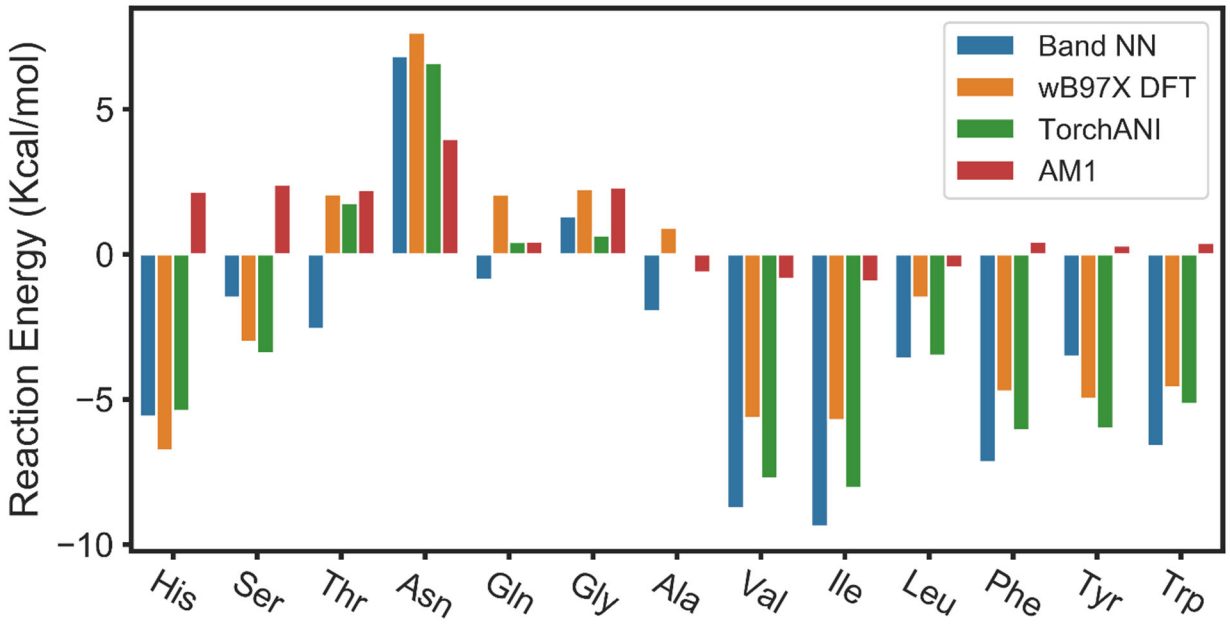

Figure 58. Reaction energy for amino acid to keto acid reactions predicted by BAND NN (Blue) and TorchANI (Green) ANNs, wB97X DFT (Orange), and semiempirical method AM1 (Red). Value predicted by wB97X is considered the target value.

4. CONCLUSION

As part of the Tactical Disablement Project, neat weapons-grade HD was reacted with lithium nitride (Li_3N) and water on a small scale (1-10 mL). Products were analyzed using ^{13}C NMR, and no reaction products were observed. This reagent combination gave excellent results for decontaminating nerve agents and precursors, but it was not effective for HD.

Other reagents were studied, including lithium aluminum hydride, mixtures of reagents based on Grignard and Friedel-Crafts chemistry, and other types of reagents. The best performance was found for $NaOCH_3$, which reacted with HD to form methoxylated products, but with a reagent ratio that did not meet the project goals.

Studies were also done of the optimal methods for making pellets of Li_3N. The chemistry of Li_3N was also studied in reactions with various alcohols and acids and with various simulants of HD. In spite of a large number of studies and reagent combinations, a method for reaction of HD was not found that met the project goals.

Finally, *ab initio* computational studied were done to indicate a wealth of information for comparing reactions that is not available experimentally. HD has a complex chemistry that can involve S_N2 and E2 reaction mechanisms, nonpolar and ionic reaction intermediates and products, and cyclic sulfonium ion intermediates. An effort to find new ways to model the chemistry could be important not only for decontamination reactions but also for understanding physiological activity. Machine learning tools were reviewed to determine which methods might be useful for modeling reactivity.

LITERATURE CITED

1. McGarvey, D.; Creasy, W.; Kinnan, M. *Characterization of Solid Reaction Products from the Reaction of VX with Li_3N+H_2O for the Tactical Disablement Project*; CCDC CBC-TR-1635; U.S. Army Combat Capabilities Development Command Chemical Biological Center: Aberdeen Proving Ground, MD, Feb. 2020. UNCLASSIFIED Report. (AD1091850).

2. McGarvey, D.; Creasey, W.; Kinnan, M. *Reaction of GB with Li_3N+H_2O for the Tactical Disablement Project*; CCDC CBC-TR-1720; U.S. Army Combat Capabilities Development Command Chemical Biological Center: Aberdeen Proving Ground, MD, Dec. 2020. UNCLASSIFIED Report (AD1118232).

3. McGarvey, D.; Creasy, W.; Kinnan, M. *Reaction of GD with Li_3N+H_2O for the Tactical Disablement Project;* DEVCOM CBC-TR-1774; U.S. Army Combat Capabilities Development Command Chemical Biological Center: Aberdeen Proving Ground, MD, Nov. 2021, UNCLASSIFIED Report (AD1152372).

4. McGarvey, D.; Creasy, W.; Kinnan, M. *Reaction of QL with $Li_3N + H_2O$ for the Tactical Disablement Project*, CCDC CBC-TR-1722; U.S. Army Combat Capabilities Development Command Chemical Biological Center: Aberdeen Proving Ground, MD, Dec. 2020, UNCLASSIFIED Report (AD1118236).

5. McGarvey, D.; Creasy, W.; Kinnan, M. *DF Reaction with $Li_3N + H_2O$ for the Tactical Disablement Project*; CCDC CBC-TR-1721; U.S. Army Combat Capabilities Development Command Chemical Biological Center: Aberdeen Proving Ground, MD, Dec. 2020, UNCLASSIFIED Report (AD1118235).

6. Mason, P.S., Jr. *Reactions of Lithium Nitride with Some Unsaturated Organic Compounds.* Ph.D. Thesis, Louisiana State University, Baton Rouge, LA, 1963. https://digitalcommons.lsu.edu/cgi/viewcontent.cgi?article=1897&context=gradschool_disstheses

7. Baldwin, F.P.; Blanchard, E.J.; Koenig, P.E. Metal Nitrides in Organic Reactions. I. Reactions of Lithium Nitride with Acid Chlorides. Preparation of N,N-Diacylamides. *J. Org. Chem*. **1965,** *30* (3), 671.

8. Chemical Datasheet Lithium Nitride. https://cameochemicals.noaa.gov/chemical/1001 (accessed April 22, 2024).

9. Mason, P.S., Jr. *Reactions of Lithium Nitride with Some Unsaturated Organic Compounds*. Ph. D. Dissertation, Louisiana State University, Baton Rouge, LA, 1963.

10. McGarvey, D.; Creasy, W.; Knoebel, R.; Kinnan, M. *Reaction of Large Volume GB with Li_3N+H_2O and Unresolved Issues for the Tactical Disablement Project*; DEVCOM CBC-TR-1804; U.S. Army Combat Capabilities Development Command Chemical Biological Center: Aberdeen Proving Ground, MD, Oct. 2022, UNCLASSIFIED Report (AD1192105).

11. Yand, Y.C.; Szafraniec, L.L.; Beaudry, W.T.; Ward, J.R. Kinetics and Mechanism of the Hydrolysis of 2-chloroethyl Sulfides. *J. Org. Chem.* **1988,** *53*, 3293–3297.

12. Harvey, S.P.; Szafraniec, L.L.; Beaudry, W.T.; Earley, J.T.; Irvine, R.L. *Neutralization and Biodegradation of Sulfur Mustard*; ERDEC-TR-388, Edgewood Research, Development, & Engineering Center: Aberdeen Proving Ground, MD, Feb. 1997, UNCLASSIFIED Report (ADA322638).

13. Demek, M.M.; Davis, G.T.; Dennis, W.H., Jr.; Hill, A L.; Farrand, R.L.; Musselman, N.P.; Mazza, R.J.; Levine, W.D.; Rosenblatt, D.H.; Epstein, J. *Behavior of Chemical Agents in Seawater;* EATR 4417, Edgewood Arsenal: Edgewood Arsenal, MD, Aug. 1970, UNCLASSIFIED report (CBRNIAC-CB-001952).

14. Lemonick, S. Simulations Unveil Grignard Reactions Complex Mechanism. *Chem. Eng. News*. **2020,** 7.

15. Peltzer, R.M.; Gauss, J.; Eisenstein, O.; Cascella, M. The Grignard Reaction-Unraveling a Chemical Puzzle. *J. Am. Chem. Soc.* **2020,** 142, 2984–2994.

16. Iwasaki, T.; Imanishi, R.; Shimizu, R.; Kuniyasu, H.; Terao, J.; Kambe, N. Copper-Catalyzed Alkyl-Alkyl Cross-Coupling Reactions Using Hydrocarbon Additives: Efficiency of Catalyst and Roles of Additives. *J. Org. Chem.* **2014,** *79* (18), 8522–8532.

17. Riley, P.C.; Willis, M.P.; Schenning, A.M. Decontamination of Sulfur Mustard by Polymerization, in *Proceedings of the Edgewood Chemical Biological Center In-House Laboratory Independent Research and Surface Science Initiative Programs FY13*, U.S. Army Edgewood Chemical Biological Center: Aberdeen Proving Ground, MD, 2013, pp.73–80, UNCLASSIFIED Report (SURVIAC-2025361).

18. Leverant, C.J.; Priest, C.W.; Greathouse, J.A.; Kinnan, M.K.; Rempe, S.B. Quantum Calculations of VX Ammonolysis and Hydrolysis Pathways via Hydrated Lithium Nitride. *Int. J. Mol. Sci.* **2021,** *22*, 08653. DOI: 10.3390/ijms22168653.

19. Priest, C.W.; Greathouse, J.A.; Kinnan, M.K.; Burton, P.D.; Rempe, S.B. Ab Initio and Force Field Molecular Dynamics Study of Bulk Organophosphorus and Organochlorine Liquid Structures. *J. Chem. Phys*. **2021,** *154*, 084503. DOI: 10.1063/5.0033426.

20. Rogers, D.; Hahn, M. Extended-Connectivity Fingerprints. *J. Chem. Inf. Model.* **2010,** 50 (5), 742–54.

21. RDKit. https://www.rdkit.org/ (accessed April 22, 2024).

22. Simplified Molecular-Input Line-Entry System. *Wikipedia.* https://en.wikipedia.org/wiki/Simplified_molecular-input_line-entry_system (accessed April 22, 2024).

23. Delaney, J.S. ESOL: Estimating Aqueous Solubility Directly from Molecular Structure. *J. Chem. Inf. Comput. Sci.* **2004,** *44* (3), 1000–5.

24. Laghuvarapu, S.; Pathak, Y.; Priyakumar, U.D. BAND NN: A Deep Learning Framework for Energy Prediction and Geometry Optimization of Organic Small Molecules. *J. Comput. Chem.* **2020,** *41* (8), 790–799.

25. Gao, X.; Ramezanghorbani, F.; Isayev, O.; Smith, J.S.; Roitberg, A.E. Torchani: A Free and Open Source Pytorch-Based Deep Learning Implementation of the Ani Neural Network Potentials. *J. Chem. Inf. Model*. **2020,** *60*, 3408–3415.

Blank

ACRONYMS AND ABBREVIATIONS

APG	Aberdeen Proving Ground
ACN	Acetonitrile
BCEE	Bis(chloroethyl) ether
CA	chemical agent
CASARM	U. S. Army Chemical Agent Standard Analytical Reference Materiel
CCDC CBC	U. S. Army Combat Capabilities Development Command Chemical Biological Center
CEES	Chloroethyl ethyl sulfide
CEPS	Chloroethyl phenyl sulfide
CTF	U. S. Army Chemical Transfer Facility
CW	chemical warfare
CWA	chemical warfare agent
DEVCOM CBC	U. S. Army Combat Capabilities Development Command Chemical Biological Center
DMMP	Dimethyl methylphosphonate
DPCP	Diphenyl chlorophosphate
HD	Bis(2-chloroethyl)sulfide
Li3N	Lithium nitride
NMR	Nuclear magnetic resonance spectroscopy
SNL	Sandia National Laboratories
TEP	Triethyl phosphate
XRD	X-ray Diffraction

Blank

DISTRIBUTION LIST

The following individuals and organizations were provided with one Adobe portable document format (pdf) electronic version of this report:

U.S. Army Combat Capabilities Development
Command Chemical Biological Center
(DEVCOM CBC)
Decontamination Sciences Branch
FCDD-CBR-PD
ATTN: McGarvey, D.
Creasy, W.
Morrissey, K.

DEVCOM CBC Technical Library
FCDD-CBR-L
ATTN: Foppiano, S.
Stein, J.

DEVCOM CBC Operational Toxicology Branch
FCDD-CBR-TO
ATTN: Knoebel, R.

Defense Technical Information Center
ATTN: DTIC OA

Defense Threat Reduction Agency
DTRA-RD-IAR
ATTN: Pate, B.

U.S. ARMY

U.S. ARMY COMBAT CAPABILITIES DEVELOPMENT COMMAND
CHEMICAL BIOLOGICAL CENTER